Exact extreme, order, and sum statistics in a class of strongly correlated systems

Marco Biroli ⬡,[1] Hernán Larralde,[2] Satya N. Majumdar,[1] and Grégory Schehr[3]

[1]*LPTMS, CNRS, Université Paris-Sud, Université Paris-Saclay, 91405 Orsay, France*
[2]*Instituto de Ciencias Físicas, UNAM, CP 62210 Cuernavaca Morelos, México*
[3]*Sorbonne Université, Laboratoire de Physique Théorique et Hautes Energies, CNRS UMR 7589, 75252 Paris Cedex 05, France*

Even though strongly correlated systems are abundant, only a few exceptional cases admit analytical solutions. In this paper we present a large class of solvable systems with strong correlations. We consider a set of N independent and identically distributed random variables $\{X_1, X_2, \ldots, X_N\}$ whose common distribution has a parameter Y (or a set of parameters) which itself is random with its own distribution. For a fixed value of this parameter Y, the X_i variables are independent and we call them conditionally independent and identically distributed. However, once integrated over the distribution of the parameter Y, the X_i variables get strongly correlated yet retain a solvable structure for various observables, such as for the sum and the extremes of X_i's. This provides a simple procedure to generate a class of solvable strongly correlated systems. We illustrate how this procedure works via three physical examples where N particles on a line perform independent (i) Brownian motions, (ii) ballistic motions with random initial velocities, and (iii) Lévy flights, but they get strongly correlated via *simultaneous resetting* to the origin. Our results are verified in numerical simulations. This procedure can be used to generate an endless variety of solvable strongly correlated systems.

I. INTRODUCTION

The study of the statistics of functions of independent random variables is central to the foundations of probability theory. In fact, the central limit theorem, which describes the sum of independent random variables, long predates modern probability theory and has led to innumerable applications and results [1]. Another observable of much interest is the statistics of the maximum (or the minimum) of a set of random variables. This is usually referred to as "extreme value statistics" (EVS). The EVS of independent random variables are also well understood [2–6] and are of a particular practical interest since, although rare, being extreme by nature these events may lead to devastating consequences. Indeed, in many contexts, such as engineering [2], environmental sciences [7], computer science [8–12], finance [13,14], or physics [4,15,16], to cite but a few, the understanding of extreme events is a matter of crucial importance. For example, in engineering and environmental sciences the statistics of rare events, such as weak components or natural disasters, may be of major importance to the endeavor at hand. Interestingly, many of. these statistics tend to universal asymptotic forms in the limit of large number of variables. Examples are, of course, the central limit theorem and the Lévy limit distributions for the sums of independent random variables. In parallel, one of the most important contribution to the field of extreme-value theory was the Fisher-Tippett-Gnedenko theorem, which universally characterized the EVS of a set of identically distributed independent random variables. The distribution of the maximum in the large-N limit converges to the one of the three possible limiting forms: Gumbel, Fréchet, or Weibull according to the behavior of the tail of the distribution of the variables. These results have been generalized for non-identically distributed independent variables [17–21] and for a large set of weakly correlated identically distributed random variables, where the results, in the large-N limit, reduce to the independent case [22]. However, only rare and punctual results are known for the statistics of strongly correlated random variables [11,22–31]. Yet many physical systems present strong correlations and a lack of universal characterization for such systems greatly hinders progress in this area.

In a recent paper [32] we introduced a model of N non-interacting Brownian motions on the line that are subjected to simultaneous resetting to the origin. This simultaneous resetting makes the N particles strongly correlated, yet it retains an exactly solvable structure. Indeed, many observables including the EVS have been computed explicitly for this model [32]. This straightforward mechanism of generating strong correlations via simultaneous resetting can actually be generalized to a wider class of systems, as we show in this paper. The EVS of strongly correlated variables are, in general, very hard to solve and there exist only few exactly solvable cases [22–31]. This generalization that we provide here opens up a wider class of solvable models with strong correlations.

The mechanism behind this generalization is straightforward. Consider a set of N independent and identically distributed random variables $X_1, \ldots, X_N$ with a common distribution which contains a set of parameters $Y_1, Y_2, \ldots, Y_M = \vec{Y}$ which themselves are random variables with their own distribution. An example of the case $N = 1$ and $M = 1$ is where X refers to the energy of a gas and Y refers for example to the temperature or the magnetic field. In this case, the statistics of X, averaged over the distribution of Y, is referred

014101-1

to as "superstatistics" and has been studied in various contexts [33–39]. For fixed values of these parameters, the X_i variables are statistically independent with a joint distribution,

$$\text{Prob.}[X_1, \ldots, X_N | \vec{Y}] = \prod_{i=1}^{N} \text{Prob.}[X_i | \vec{Y}]. \qquad (1)$$

Hence we call these X_i variables conditionally independent and identically distributed random variables. However, when one integrates over the Y_i variables, the joint distribution of $X_1, X_2, \ldots, X_N$ is no longer factorizable,

$$\text{Prob.}[X_1, \ldots, X_N] = \int \left\{ \prod_{i=1}^{N} \text{Prob.}[X_i | \vec{Y}] \right\} \text{Prob.}[\vec{Y}] \, d\vec{Y}. \quad (2)$$

Thus the X_i's get correlated since they share the same set of parameters $\vec{Y}$. A physical example of such a system is provided by a simplified version of models of "diffusing diffusivity" where N Brownian motions $X_1(t), \ldots, X_N(t)$ share a common diffusion constant $Y_1 = D$ [40,41] which does not evolve in time but is randomly initialized. In this specific case, Eq. (2) would read

$$\text{Prob.}[X_1(t), \ldots, X_N(t)] = \int \left\{ \prod_{i=1}^{N} \frac{1}{\sqrt{4\pi Dt}} \exp\left[-\frac{X_i(t)^2}{4Dt} \right] \right\}$$
$$\times \text{Prob.}[D] \, dD. \qquad (3)$$

This example clearly demonstrates that the joint distribution of X_i's does not factorize and hence the X_i variables are correlated. Many other physical examples motivated by stochastic resetting will be discussed in this paper, but this family of systems describes a wide variety of physical problems. We provide here a short nonexhaustive list of such problems so that the reader may grasp the type of problems which can be described by this protocol. This protocol can be used to describe the following:

(i) the statistics of N independent stochastic processes measured after a random time $Y = T$.

(ii) the statistics of N experimental observations $X_1, \ldots, X_N$ which depend on some experimental parameters $Y_1, \ldots, Y_M$ that may have some non-negligible uncertainties $\sigma_1, \ldots, \sigma_M$. Then, supposing we know $\text{Prob.}[X_i | \vec{Y}]$, we can model $\text{Prob.}[\vec{Y}]$ by a M Gaussians centered around their expected values and with variances $\vec{\sigma}$.

(iii) the statistics of N independent particles $X_1, \ldots, X_N$ evolving in an energy landscape $E(Y_1, \ldots, Y_M)$ which depends on some parameters $Y_1, \ldots, Y_M$ (magnetization, temperature, etc.) which are randomly initialized according to some distribution at $t = 0$.

A natural question is whether it is possible to generalize the well-known results of certain observables for independent and identically distributed random variables, such as the sum or the EVS, to the conditionally independent and identically distributed variables. For example, for N independent and identically distributed variables, it is known that the rescaled sum (sometimes referred to as the "sample mean") $C = \frac{1}{N} \sum_{i=1}^{N} X_i$ converges to a Gaussian random variable in the large-N limit: This is the celebrated central limit theorem (CLT) [42]. How does the CLT get modified for conditionally independent and identically distributed variables? Similarly,

as mentioned before, the EVS of N independent and identically distributed random variables, appropriately centered and scaled, converges for large N, to one of the three limiting distributions Gumbel, Fréchet, and Weibull. Are there similar limiting universal distributions for conditionally independent and identically distributed variables? After recalling these results for independent and identically distributed variables in Sec. II, we will consider their generalizations to conditionally independent and identically distributed variables in Sec. III.

Once these general results are elucidated, it is natural to look for examples in physical systems where the conditionally independent and identically distributed variables arise naturally. As mentioned earlier, the case of N Brownian motions on a line, all starting at the origin at $t = 0$ and are simultaneously reset to the origin with rate r, provides a natural example of such conditionally independent and identically distributed variables [32]. For a typical realization of this process for $N = 3$ particles, see the left panel of Fig. 1. In this case, it was shown that the joint distribution of the positions approaches a nonequilibrium stationary state given by [32]

$$\text{Prob.}[X_1, \ldots, X_N] = \int_0^{\infty} \left\{ \prod_{i=1}^{N} \frac{1}{\sqrt{4\pi D\tau}} e^{-\frac{X_i^2}{4D\tau}} \right\} (re^{-r\tau}) \, d\tau. \tag{4}$$

A detailed derivation of this result is provided in Sec. IV A, where we show that the EVS for this conditionally independent and identically distributed model can be computed exactly. Note that without the averaging over τ, i.e., for a fixed τ, the X_i's are independent and identically distributed variables, each distributed via a Gaussian. Hence for fixed τ, their EVS converges to the Gumbel limiting distribution. Therefore this example provides a generalization of the Gumbel class to conditionally independent and identically distributed variables. It is natural to ask whether there are physical models of conditionally independent and identically distributed variables whose independent and identically distributed counterparts have EVS belonging to the other two universality classes, namely the Fréchet and the Weibull classes. In fact, we introduce two new models of N independent particles on a line that precisely do this job. For the Weibull class, we consider a model of N independent ballistic particles, all starting at the origin with random velocities v_i's each drawn independently from a uniform distribution $v_i \in [-1, +1]$, that are simultaneously reset to the origin with rate r. After every resetting, the velocities are also renewed. For a typical realization of this ballistic resetting process for $N = 3$ particles, see the middle panel in Fig. 1. We show that the EVS for this conditionally independent and identically distributed model can also be computed exactly. Finally, we study a conditionally independent and identically distributed model whose independent and identically distributed counterpart corresponds to the Fréchet class for the EVS. In this model, we consider N independent Lévy flights, all starting at the origin and are reset simultaneously to the origin with rate r. In the rightmost panel of Fig. 1, a typical realization of this process for $N = 3$ is shown. For this model also, we show that the EVS can be computed exactly, despite the fact that the system is strongly correlated.
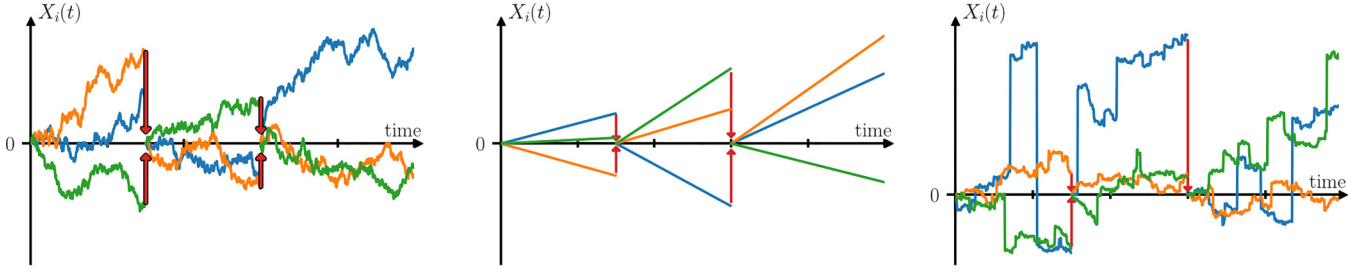
FIG. 1. A typical realization of three simultaneously resetting processes for $N = 3$ particles (with different colors): (i) N Brownian motions on a line, belonging to the Gumbel class of conditionally independent and identically distributed variables, (ii) N ballistic particles on a line, with random velocities drawn from a uniform distribution over $[-1, +1]$, belonging to the Weibull class of conditionally independent and identically distributed variables, and (iii) N Lévy flights on a line, belonging to the Fréchet class of conditionally independent and identically distributed variables. The red vertical arrows indicate the simultaneous resetting events.

The rest of the paper is organized as follows. In Sec. II we recall the well-known results for the independent and identically distributed variables. The conditionally independent and identically distributed variables are introduced in Sec. III. The results for the rescaled sum of conditionally independent and identically distributed variables are given in Sec. III while the derivations are detailed in the Appendix. The EVS for general conditionally independent and identically distributed variables are studied Sec. III B. The three physical models are introduced and analyzed in Sec. IV. Finally, we conclude in Sec. V.

II. KNOWN RESULTS FOR INDEPENDENT AND IDENTICALLY DISTRIBUTED RANDOM VARIABLES

The statistics of independent and identically distributed random variables have been widely studied and are fully understood. We recall in this section the known results for the order statistics and the extreme value statistics of independent and identically distributed variables [5,6,22,43,44]. We consider N independent and identically distributed variables $X_1, \ldots, X_N$ each distributed via $p(X)$ and we denote their cumulative distribution function by $P(X) = \text{Prob.}[X_i \leqslant X]$. We define the order statistics by sorting them in decreasing order of magnitude

$$X_{\max} = M_{1,N} \geqslant M_{2,N} > \cdots > M_{N,N} = X_{\min}, \quad (5)$$

where $X_{\max}$ (respectively, $X_{\min}$) denotes the maximum (respectively, minimum) among the $X_i's$. We define the cumulative distribution function of the kth maximum,

$$F_{k,N}(w) = \text{Prob.}[M_{k,N} \leqslant w]. \quad (6)$$

When $k = O(N)$, we will refer to $M_{k,N}$ as the "bulk" order statistics, while the case $k = O(1)$ will be referred to as the extremes at the "edge." In particular, the case $k = 1$, i.e., the distribution of the global maximum $M_{1,N}$, will be referred to as the EVS.

We start by characterizing the maximum, i.e., $X_{\max} = M_{1,N}$ which corresponds to $k = 1$. In this case, the cumulative distribution function (appropriately centered and scaled) converges to a limiting scaling form

$$F_{1,N}(w) \xrightarrow[N \to +\infty]{} G_\rho \left(\frac{w - a_N}{b_N} \right). \quad (7)$$

The scale factors a_N and b_N depend on the details of the probability distribution function (p.d.f.) $p(x)$. However, it turns out that the scaling function $G_\rho(z)$ can be only of three varieties labeled by $\rho = $ I, II, III (respectively the Gumbel, the Fréchet, and the Weibull). When $N \to \infty$, the cumulative distribution function $F_{1,N}(w)$ converges to one of these three scaling functions, depending on the tail of $p(x)$ as discussed below.

A. The Gumbel universality class

If the p.d.f. $p(X)$ decays faster than any power law for large X, i.e., when $X \gg 1$, then $p(X) \ll X^{-\eta}$ for any $\eta > 0$, then $p(X)$ is said to belong to the Gumbel universality class. In this case

$$G_{\text{I}}(z) = e^{-e^{-z}}, \quad \int_{a_N}^{+\infty} p(X) dX = \frac{1}{N}$$

$$\text{and} \quad b_N = N \int_{a_N}^{+\infty} (x - a_N) p(X) dX. \quad (8)$$

The scaling factors a_N and b_N are fixed by the last two equations in Eq. (8).

B. The Fréchet universality class

If the p.d.f. $p(X)$ has an unbounded support and decays as a power law for large X, i.e., when $X \gg 1$, then $p(X) \propto X^{-1-\mu}$ for a given $\mu > 0$, then $p(X)$ is said to belong to the Fréchet universality class. In this case

$$G_{\text{II}}(z) = \Theta(z) e^{-z^{-\mu}}, \quad a_N = 0 \text{ and } \int_{b_N}^{+\infty} p(X) dX = \frac{1}{N}, \quad (9)$$

where $\Theta(z)$ is the Heaviside distribution.

C. The Weibull universality class

If the p.d.f. $p(X)$ has a support bounded from above at $X^\star$ and decays as a power law when approaching $X^\star$, i.e., when $X^\star - X \ll 1$, then $p(X) \propto (X^\star - X)^{\mu-1}$ for a given $\mu > 0$, then $p(X)$ is said to belong to the Weibull universality

class. In this case

$$G_{\text{III}}(z) = \begin{cases} 1, & z > 0, \\ e^{-|z|^\mu}, & z < 0, \end{cases} \quad a_N = X^\star \text{ and } \int_{X^\star-b_N}^{X^\star} p(X)dX = \frac{1}{N}. \tag{10}$$

With these three classes we have universally characterized the EVS of independent and identically distributed variables.

It turns out that the cumulative distribution function of the kth maximum $M_{k,N}$ when $k = O(1)$ can also be expressed in terms of the three scaling functions $G_\rho(z)$,

$$\text{Prob.}(M_{k,N} \leqslant w) \xrightarrow[N \to +\infty]{} \mathcal{F}_\rho^k\left(\frac{w - a_N}{b_N}\right), \tag{11}$$

with the scaling function

$$\mathcal{F}_\rho^k(z) = \frac{1}{\Gamma(k)} \int_{-\log G_\rho(z)}^{+\infty} e^{-t} t^{k-1} dt, \quad \rho = \text{I, II, III}, \tag{12}$$

where $\Gamma(z)$ is the Gamma function. For $k = 1$, one can easily check that $\mathcal{F}_\rho^{k=1}(z) = G_\rho(z)$. When $k = O(N)$, i.e., one is probing the order statistics $M_{k,N}$ in the "bulk," the large-N limiting form of the p.d.f. of $M_{k,N}$ is known to be a Gaussian [5,6],

$$\text{Prob.}[M_{k=\alpha N,N} = w] \xrightarrow[N \to +\infty]{} \sqrt{\frac{Np[q(\alpha)]^2}{2\pi\alpha(1-\alpha)}}$$

$$\times \exp\left\{-\frac{Np[q(\alpha)]^2}{2\alpha(1-\alpha)}[w - q(\alpha)]^2\right\}. \tag{13}$$

where $0 < \alpha < 1$ and $q(\alpha)$ is the α quantile obtained implicitly from

$$\int_{q(\alpha)}^{+\infty} p(X) \, dX = \alpha. \tag{14}$$

The quantile $q(\alpha)$ denotes the value of X_i such that there are, on an average, αN variables above $q(\alpha)$.

III. CONDITIONALLY INDEPENDENT AND IDENTICALLY DISTRIBUTED RANDOM VARIABLES

We recall from Eq. (2) that the joint distribution of N conditionally independent and identically distributed variables conditioned on $\vec{Y} = \{Y_1, Y_2, \ldots, Y_M\}$ is given by

$$\text{Prob.}[X_1, \ldots, X_N] = \int \left\{\prod_{i=1}^N p(X_i|\vec{Y})\right\} h(\vec{Y}) \, dY_1 \cdots dY_M, \tag{15}$$

where $p(X_i|\vec{Y}) = \text{Prob.}(X_i|Y_1, Y_2, \ldots, Y_M)$ is the conditional p.d.f. of X_i and $h(\vec{Y})$ denotes the joint distribution of $\vec{Y} = \{Y_1, Y_2, \ldots, Y_M\}$. It is clear from Eq. (15) that the joint p.d.f. of X_i's is not factorizable in general. Hence the X_i's are correlated. By choosing $h(\vec{Y})$, one can generate a wide class of such correlated variables. To analyze the nature of the correlations, it is convenient to compute the connected correlator $\langle X_i^n X_j^n \rangle - \langle X_i^n \rangle \langle X_j^n \rangle$, for a generic n. To compute this, we first

need the nth moment $\langle X_i^n \rangle$, which is simply

$$\langle X_i^n \rangle = \int d\vec{X} \, X_i^n \, \text{Prob.}[\vec{X}]$$

$$= \int d\vec{X} \, X_i^n \int d\vec{Y} \, h(\vec{Y}) \prod_{k=1}^N p(X_k|\vec{Y}), \tag{16}$$

where $\vec{X} = \{X_1, X_2, \ldots, X_N\}$ and $d\vec{X} = dX_1 dX_2 \cdots dX_N$. Consequently, the connected correlator is given by

$$\langle X_i^n X_j^n \rangle - \langle X_i^n \rangle \langle X_j^n \rangle = \int d\vec{Y} \, h(\vec{Y}) \int d\vec{X} X_i^n X_j^n \prod_{k=1}^N p(X_k|\vec{Y})$$

$$- \langle X_i^n \rangle \langle X_j^n \rangle, \tag{17}$$

where $\langle X_i^n \rangle$ is given in Eq. (16). For a generic $h(\vec{Y})$, this connected correlator is nonzero, indicating the presence of all-to-all correlations between the X_i variables, which thus make them strongly correlated.

A. The scaled sum of conditionally independent and identically distributed variables

The main focus of this paper is on the order and the extreme statistics for conditionally independent and identically distributed variables that we discuss in detail in the later sections. However, it is also of interest to compute the statistics of the sum of such conditionally independent and identically distributed variables and to explore if there is an equivalent to the central limit theorem or Lévy stable theorem for the conditionally independent and identically distributed case. In order not to shift the focus away from the order and the extreme statistics, in this section we present only the main results for the statistics of the sum and provide the detailed derivations in the Appendix.

Let us now summarize the main results for the rescaled sum $C = \frac{1}{N} \sum_{i=1}^N X_i$ of conditionally independent and identically distributed variables $X_1, \ldots, X_N$. We defer the derivation of these results to the Appendix. If the conditional distribution $p(X_i|\vec{Y})$ admits a finite first moment $m(\vec{Y})$ which is a nonconstant function of $\vec{Y}$ and a finite second moment $\sigma(\vec{Y})$, then the p.d.f. $P(C, N)$ of the rescaled sum can be written as

$$P(C, N) \xrightarrow{N \to +\infty} \int d\vec{Y} \, \delta(m(\vec{Y}) - C) \, h(\vec{Y}). \tag{18}$$

On the other hand, if $m(\vec{Y}) = m$ is a constant, then

$$P(C, N) \xrightarrow{N \to +\infty} \sqrt{N}\mathcal{P}[(C - m)\sqrt{N}], \text{ where } \mathcal{P}(Z)$$

$$= \frac{1}{\sqrt{2\pi}} \int \frac{d\vec{Y}}{\sigma(\vec{Y})} \exp\left[-\frac{Z^2}{2\sigma^2(\vec{Y})}\right] h(\vec{Y}). \tag{19}$$

Finally, if $p(X_i|\vec{Y})$ does not admit a finite first or second moment and instead has a power-law tail $p(X_i|\vec{Y}) \sim 1/X^{1+\mu}$

for large X, with $0 < \mu < 2$, then

$$P(C, N) \approx N^{1-1/\mu} \mathcal{P}_\mu \left(\frac{C}{N^{1/\mu-1}} \right) \text{ where } \mathcal{P}_\mu(Z)$$

$$= \int \frac{d\vec{Y}}{b(\vec{Y})} \mathcal{L}_\mu \left[\frac{Z}{b(\vec{Y})} \right] h(\vec{Y}), \tag{20}$$

where $\mathcal{L}_\mu(z)$ is the Lévy stable distribution (scaled to unity) [45]

$$\mathcal{L}_\mu(z) = \int_{-\infty}^{\infty} \frac{dq}{2\pi} e^{-iqz-|q|^\mu}. \tag{21}$$

It has the asymptotic behaviors [45]

$$\mathcal{L}_\mu(z) \approx \begin{cases} \frac{1}{\pi\mu} \Gamma(1/\mu), & z \to 0, \\ \frac{1}{z^{1+\mu}} \sin\left(\frac{\pi\mu}{2}\right) \frac{\Gamma(\mu+1)}{\pi} & z \to \infty. \end{cases} \tag{22}$$

B. Order statistics of conditionally independent and identically distributed variables

In this section, we provide a complete characterization of the order statistics and EVS for conditionally independent and identically distributed variables. We consider again a set of N conditionally independent and identically distributed random variables $X_1, \cdots, X_N$. Since the X_i's are conditionally independent, the p.d.f. of the kth maxima $M_{k,N}$ conditioned on $\vec{Y}$ is given by

$$\text{Prob.}[M_{k,N} = w|\vec{Y}] = \frac{N!}{(k-1)!(N-k)!} p(w|\vec{Y})$$

$$\times \left[\int_w^{+\infty} p(X|\vec{Y}) dX \right]^{k-1}$$

$$\times \left[\int_{-\infty}^w p(X|\vec{Y}) dX \right]^{N-k}. \tag{23}$$

This equation is exact for any k and any distribution $p(X|\vec{Y})$ and can be understood as follows. For the kth maximum to be located at w, we need to place one variable exactly at w, $k-1$ variables above w and $N-k$ variables below w. The p.d.f. of the kth maximum, integrated over $\vec{Y}$, reads

$$\text{Prob.}[M_{k,N} = w] = \int d\vec{Y} \, h(\vec{Y}) \, \text{Prob.}[M_{k,N} = w|\vec{Y}]. \tag{24}$$

We now study the large-N limit of this p.d.f. by setting $k = \alpha N$ where $0 < \alpha < 1$. Equation (23) then gives

$$\text{Prob.}[M_{k,N} = w|\vec{Y}] = \frac{\Gamma(N+1)}{\Gamma(\alpha N)\Gamma[N(1-\alpha)+1]}$$

$$\times \frac{p(w|\vec{Y})}{\int_w^{+\infty} p(X|\vec{Y}) dX} e^{-N\Phi_\alpha(w)}, \tag{25}$$

where we rewrote the combinatorial factor using the Gamma function $\Gamma(z)$ and we introduced the function

$$\Phi_\alpha(w) = -\alpha \ln \left[\int_w^{+\infty} p(X|\vec{Y}) dX \right]$$

$$- (1-\alpha) \ln \left[\int_{-\infty}^w p(X|\vec{Y}) dX \right]. \tag{26}$$

So far, we have not taken the large-N limit. When $N \to \infty$, the p.d.f. in (25) gets sharply concentrated around the value $w = q(\alpha, \vec{Y})$ that minimizes $\Phi_\alpha(w)$. Setting $\Phi'_\alpha[w = q(\alpha, \vec{Y})] = 0$ yields

$$\int_{q(\alpha,\vec{Y})}^{+\infty} p(X|\vec{Y}) \, dX = \alpha. \tag{27}$$

Notice that this corresponds to the definition of the α quantile of the conditional distribution $p(X|\vec{Y})$. Then expanding $\Phi_\alpha(w)$ around $q(\alpha, \vec{Y})$ up to quadratic order, one finds that for large N and close to $q(\alpha, \vec{Y})$, the p.d.f. defined in Eq. (25) simplifies to

$$\text{Prob.}[M_{k,N} = w|\vec{Y}] \approx \sqrt{\frac{N[p(q\,|\,\vec{Y})]^2}{2\pi\alpha(1-\alpha)}}$$

$$\times \exp \left\{ -\frac{N[p(q\,|\,\vec{Y})]^2}{2\alpha(1-\alpha)} [w-q]^2 \right\}, \tag{28}$$

where for brevity we suppressed the explicit dependence on α and $\vec{Y}$ of $q \equiv q(\alpha, \vec{Y})$. Then Eq. (28) is simply a Gaussian distribution centered around q with variance

$$\text{Var} = \frac{\alpha(1-\alpha)}{N[p(q\,|\,\vec{Y})]^2}. \tag{29}$$

For the order statistics in the bulk where $\alpha \sim \mathcal{O}(1)$, it follows from Eq. (27) that $q(\alpha, \vec{Y})$ is also of order $\mathcal{O}(1)$. Consequently, from Eq. (29), one finds that $\text{Var} \sim \mathcal{O}(1/N)$. Under these conditions, in the large-N limit, the p.d.f. in Eq. (28) becomes sharply peaked and can be approximated by a Dirac delta function centered at $q(\alpha, \vec{Y})$. Note that this is true regardless of the underlying distribution $p(X|\vec{Y})$. Substituting the Dirac delta function back in Eq. (24), we find that the p.d.f. of the kth maximum in the bulk converges, in the large-N limit, to an N-independent limiting form given by

$$\text{Prob.}[M_{k,N} = w] \xrightarrow[N\to\infty]{} \int d\vec{Y} \, h(\vec{Y}) \, \delta[w - q(\alpha, \vec{Y})]. \tag{30}$$

This result characterizes the order statistics in the bulk for conditionally independent and identically distributed variables.

However, for the order statistics near the edge, where $\alpha = \mathcal{O}(1/N)$, we need to carefully study the dependence on N of the quantile $q(\alpha, \vec{Y})$ and the variance Var. From Eq. (27) we see that when $\alpha \sim \mathcal{O}(1/N) \ll 1$, the quantile $q(\alpha, \vec{Y})$ depends on the tail of $p(X|\vec{Y})$ for large X. We therefore analyze separately the three classes of tails that lead to the three universality classes of the EVS in the independent and identically distributed case. In Sec. III B 1, we study the Gumbel class, where the distribution $p(X|\vec{Y})$ decays faster than a power law for large X. In Section III B 2, we study the Weibull class, where the support of the distribution $p(X|\vec{Y})$ is bounded above and approaches its upper bound as a power law. Finally, in Sec. III B 3, we study the Fréchet class, where the distribution $p(X|\vec{Y})$ has an unbounded support and decays as a power law for large X. We will see that while the bulk result in Eq. (30) can be extrapolated to the edge [where $k = \mathcal{O}(1)$] for the Gumbel and the Weibull class, the same cannot be done for

the Fréchet case. In the Fréchet case, the order statistics at the edge needs to be analyzed separately.

1. Edge order statistics for the Gumbel class

We start by studying random variables belonging to the Gumbel class, e.g., when the tail of the distribution $p(X_i|\vec{Y})$ decays as

$$p(X_i|\vec{Y}) \underset{X_i \gg 1}{\sim} A(\vec{Y})e^{-B(\vec{Y})X_i^{\mu(\vec{Y})}}, \tag{31}$$

where $A(\vec{Y})$, $B(\vec{Y})$, and $\mu(\vec{Y}) > 0$ are positive real functions of $\vec{Y}$. For simplicity, we will drop the explicit dependence on $\vec{Y}$ of $A(\vec{Y})$, $B(\vec{Y})$, and $\mu(\vec{Y})$ and simply denote them by A, B, and μ. In order to probe the behavior of the extremes near the edge, i.e., of $M_{k,N}$ for $k \sim \mathcal{O}(1)$. To do so, we start by studying the dependence on N of the quantile $q(\alpha, \vec{Y})$ when $\alpha = k/N = \mathcal{O}(1/N)$. From Eq. (27) we see that when $\alpha \ll 1$ then necessarily $q(\alpha, \vec{Y}) \gg 1$. Hence, in Eq. (27), we can replace the integrand by its tail behavior (31) and obtain

$$\alpha \approx \int_{q(\alpha,\vec{Y})}^{+\infty} A\, e^{-Bx^\mu}\, dx = \frac{A}{\mu B^{1/\mu}} \int_{Bq^\mu(\alpha,\vec{Y})}^{+\infty} t^{1/\mu-1}\, e^{-t}\, dt$$

$$\underset{q(\alpha,\vec{Y}) \gg 1}{\approx} \frac{A}{B\,\mu}\, q^{1-\mu}(\alpha, \vec{Y})\, e^{-B\,q^\mu(\alpha,\vec{Y})}. \tag{32}$$

where we approximated the integral by its value at its lower bound which is the leading-order contribution due to the exponential decay of the integrand. Since we are at the edge, where $\alpha = k/N \ll 1$ and $q(\alpha, \vec{Y}) \gg 1$, the leading-order solution for $q(\alpha, \vec{Y})$ from Eq. (32) is given by

$$q(\alpha, \vec{Y}) \underset{\alpha \to 0}{\approx} \frac{1}{B^{1/\mu}} \log^{1/\mu}\left(\frac{A}{B\alpha\mu}\right). \tag{33}$$

Replacing $\alpha = k/N$ with $k \sim \mathcal{O}(1)$ fixed and taking $N \to +\infty$ we obtain

$$q(\alpha, \vec{Y}) \approx \frac{1}{B^{1/\mu}} \log^{1/\mu}\left(N \frac{A}{Bk\mu}\right) \sim \mathcal{O}[\log^{1/\mu}(N)], \tag{34}$$

thus justifying *a posteriori* that $q(\alpha, \vec{Y}) \gg 1$ for large N. We now investigate how the variance Var in Eq. (29) depends on N for large N. To do so, we substitute Eq. (34) back into Eq. (31), yielding

$$p(q\,|\,\vec{Y}) \underset{\alpha \ll 1}{\approx} \frac{Bk\mu}{N}. \tag{35}$$

Using Eq. (35) in Eq. (29), we get that the variance is given by

$$\text{Var} = \frac{\alpha(1-\alpha)}{N[p(q\,|\,\vec{Y})]^2} \approx \frac{k/N}{N\left(\frac{Bk\mu}{N}\right)^2} \approx \frac{1}{B^2\mu^2 k} \sim \mathcal{O}(1). \tag{36}$$

Thus, the variance Var $= \mathcal{O}(1)$ while from Eq. (34) the mean $q(\alpha, \vec{Y}) = \mathcal{O}([\log N]^{1/\mu})$. Hence, we can write

$$M_{k,N} \approx q(\alpha, \vec{Y}) + \eta_k, \tag{37}$$

where η_k is a random variable of order $\mathcal{O}(1)$. Therefore, in the large-N limit, the fluctuations are negligible compared to the mean for any positive $A(\vec{Y})$, $B(\vec{Y})$, and $\mu(\vec{Y})$. For large N, the kth maximum $M_{k,N}$ effectively concentrates on its mean value $M_{k,N} \approx q(\alpha, \vec{Y}) \sim \log^{1/\mu}(N)$. Thus, the approximation

used to obtain Eq. (30) is still valid even at the edge, i.e., for $\alpha \sim \mathcal{O}(1/N)$. Hence, for the Gumbel class, Eq. (30) characterizes both the order statistics in the bulk as well as at the edge for conditionally independent and identically distributed variables.

2. Edge order statistics for the Weibull class

We now turn our attention to conditionally independent and identically distributed variables belonging to the Weibull class. In this case, the support of the distribution $p(X_i|\vec{Y})$ is bounded above by $x^\star(\vec{Y})$ and approaches this bound with a power-law tail given by

$$p(X_i|\vec{Y}) \underset{X_i \to x^\star(\vec{Y})}{\approx} A(\vec{Y})[x^\star(\vec{Y}) - X_i]^{\mu(\vec{Y})-1}, \tag{38}$$

for X_i close to $x^\star(\vec{Y})$, where $A(\vec{Y})$, $x^\star(\vec{Y})$, $\mu(\vec{Y}) > 0$ are positive real functions of $\vec{Y}$, where for simplicity we will drop the explicit dependence on $\vec{Y}$. We start by studying the dependence on N of the quantile $q(\alpha, \vec{Y})$. Once again, to probe the EVS we have to fix $k \sim \mathcal{O}(1)$ while taking $N \to +\infty$ to study the behavior close to the global maximum $M_{1,N}$. Hence $\alpha \sim \mathcal{O}(1/N) \ll 1$ and $q(\alpha, \vec{Y})$ must be approaching $x^\star$ from below. This justifies using the tail expression given in Eq. (38) inside the integral in Eq. (27). Hence,

$$\alpha = \int_{q(\alpha,\vec{Y})}^{+\infty} p(X|\vec{Y})\, dX = A \int_{q(\alpha,\vec{Y})}^{x^\star} (x^\star - X)^{\mu-1} dX$$

$$= \frac{A}{\mu}\,[x^\star - q(\alpha, \vec{Y})]^\mu, \tag{39}$$

which gives

$$q(\alpha, \vec{Y}) = x^\star - \left(\frac{\alpha\mu}{A}\right)^{1/\mu}. \tag{40}$$

In the limit of $N \to +\infty$, keeping $k \sim \mathcal{O}(1)$ fixed, $\alpha = k/N \to 0$ and therefore $q(\alpha, \vec{Y}) \sim \mathcal{O}(1)$. We now study the dependence on N of the variance Var. Plugging Eq. (40) back into Eq. (38) we get

$$p(q\,|\,\vec{Y}) \approx A^{1/\mu}(\alpha\mu)^{1-1/\mu}. \tag{41}$$

Thus, the variance in Eq. (29), is given by

$$\text{Var} = \frac{\alpha(1-\alpha)}{N[p(q\,|\,\vec{Y})]^2} \approx \frac{k/N(1-k/N)}{NA^{2\mu}(k\mu/N)^{2-2/\mu}}$$

$$\approx \frac{k}{A^{2\mu}(k\mu)^{2-2/\mu}} N^{-2\mu} \sim \mathcal{O}(N^{-2\mu}), \tag{42}$$

where we used $\alpha = k/N$ and took the EVS limit of $N \to +\infty$ keeping $k = \mathcal{O}(1)$ fixed. From Eqs. (40) and (42) we see that the mean is of order $\mathcal{O}(1)$ while the variance is of order $\mathcal{O}(N^{-2\mu})$. Hence the approximation that the Gaussian is sharply peaked holds and the result derived in Eq. (30) is valid for any k. Hence, for the Weibull class, Eq. (30) also fully characterizes both the order statistics in the bulk as well as at the edge for conditionally independent and identically distributed random variables.

3. Edge order statistics for the Fréchet class

Finally, we turn our attention to conditionally independent and identically distributed variables belonging to the Fréchet class. The conditional distribution $p(X_i|\vec{Y})$ has an unbounded support with a power-law tail given by

$$p(X_i|\vec{Y}) \underset{X_i \gg 1}{\approx} \frac{A(\vec{Y})}{X_i^{1+\mu(\vec{Y})}}, \qquad (43)$$

where $A(\vec{Y}) > 0$ and $2 > \mu(\vec{Y}) > 0$ are positive real functions of $\vec{Y}$. Once more, we drop the explicit dependence on $\vec{Y}$ of $A(\vec{Y})$ and $\mu(\vec{Y})$ for brevity and we will restore it later. To probe the EVS, we have to take the limit of $N \to +\infty$ keeping $k = \mathcal{O}(1)$ fixed to study the behavior close to the global maximum $M_{1,N}$. In this limit, $\alpha = k/N = \mathcal{O}(1/N) \ll 1$, which from Eq. (27) implies $q(\alpha, \vec{Y}) \gg 1$. Therefore, the integrand in Eq. (27) can be replaced by its tail behavior given in Eq. (43). Then,

$$\alpha \approx \int_{q(\alpha,\vec{Y})}^{+\infty} A \frac{dX}{X^{1+\mu}} \approx \frac{A}{\mu} q^{-\mu}(\alpha, \vec{Y}), \qquad (44)$$

hence

$$q(\alpha, \vec{Y}) \approx \left(\frac{A}{\mu\alpha} \right)^{1/\mu}. \qquad (45)$$

Taking, $\alpha = k/N$ and the limit $N \to +\infty$ keeping $k = \mathcal{O}(1)$ fixed results in

$$q(\alpha, \vec{Y}) \approx \left(\frac{AN}{\mu k} \right)^{1/\mu} \sim \mathcal{O}(N^{1/\mu}). \qquad (46)$$

This characterizes the dependence on N of the quantile $q(\alpha, \vec{Y})$. We now turn our attention to the dependence on N of the variance Var. Plugging Eq. (46) back in Eq. (43) we get

$$p(q\,|\,\vec{Y}) \underset{\alpha \ll 1}{\approx} A^{1/\mu}(\alpha)^{1/\mu+1} \approx \frac{A^{1/\mu}k^{1/\mu+1}}{N^{1/\mu+1}}, \qquad (47)$$

where we used $\alpha = k/N$. Then the variance in Eq. (29) is given by

$$\mathrm{Var} = \frac{\alpha(1-\alpha)}{N[p(q\,|\,\vec{Y})]^2} \sim \mathcal{O}(N^{2/\mu}). \qquad (48)$$

Thus the width of the fluctuations is of the same order as the mean value for large N, since $\mathrm{Var}/q(\alpha, \vec{Y})^2 \sim \mathcal{O}(1)$ and hence the distribution does not concentrate on its mean for large N—at variance with the Gumbel and the Weibull class. Thus in the Fréchet case, we need to analyze the extremes at the edge directly from the limiting behavior given in Eq. (11), instead of extrapolating the bulk result to the edge. We recall the result in Eq. (11) for $\rho = \mathrm{II}$ corresponding to the Fréchet class. It reads, for $k \sim O(1)$,

$$\mathrm{Prob.}[M_{k,N} \leqslant w\,|\,\vec{Y}] \approx \mathcal{F}_{\mathrm{II}}^k \left(\frac{w - a_N}{b_N} \right), \qquad (49)$$

where $\mathcal{F}_{\mathrm{II}}^k(z)$ is given in Eq. (12). From Eq. (9), we know that the scale factors are given by

$$a_N = 0 \text{ and } \int_{b_N}^{+\infty} p(X|\vec{Y})dX = \frac{1}{N}. \qquad (50)$$

Comparing Eq. (50) with Eq. (27) we see immediately that

$$b_N = q(1/N, \vec{Y}) \equiv q_N(\vec{Y}). \qquad (51)$$

Putting the scale factors obtained in Eq. (50) in Eq. (11) we get

$$\mathrm{Prob.}[M_{k,N} \leqslant w\,|\,\vec{Y}] \xrightarrow[N \to +\infty]{} \frac{1}{\Gamma(k)} \int_{w^{-\mu}q_N(\vec{Y})^\mu}^{+\infty} dt\ e^{-t}t^{k-1}. \qquad (52)$$

where we used $G_{\mathrm{II}}(z) = \Theta(z)\,e^{-z^{-\mu}}$ from Eq. (9).

Once again, in the $N \gg 1$ limit, we have $q_N(\vec{Y}) \gg 1$, so we can plug the tail behavior given in Eq. (43) into Eq. (50) and solve for $q_N(\vec{Y})$, as was done before for $q(\alpha, \vec{Y})$. This yields

$$q_N(\vec{Y}) \simeq \left(\frac{AN}{\mu} \right)^{1/\mu}. \qquad (53)$$

Now, using Eq. (52) in Eq. (24), we get

$$\begin{aligned} \mathrm{Prob.}[M_{k,N} \leqslant w] &= \int d\vec{Y}\ h(\vec{Y})\mathrm{Prob.}[M_{k,N} \leqslant w\,|\,\vec{Y}] \\ &= \frac{1}{\Gamma(k)} \int d\vec{Y}\ h(\vec{Y}) \int_{w^{-\mu}q_N(\vec{Y})^\mu}^{+\infty} dt\ e^{-t}t^{k-1}. \end{aligned} \qquad (54)$$

We denote the lower bound of the integral over t by

$$\lambda_N(w, \vec{Y}) = \left[\frac{q_N(\vec{Y})}{w} \right]^{\mu(\vec{Y})} = \frac{A(\vec{Y})N}{\mu(\vec{Y})w^{\mu(\vec{Y})}}, \qquad (55)$$

where we restored the explicit dependence of A and μ on $\vec{Y}$. Next we express the integral over t as

$$\begin{aligned} \int_{\lambda_N(w,\vec{Y})}^{+\infty} dt\ e^{-t}\,t^{k-1} &= \Gamma(k) - \int_0^{\lambda_N(w,\vec{Y})} dt\ e^{-t}t^{k-1} \\ &= \Gamma(k) - \int_0^\infty dt\ \Theta[\lambda_N(w,\vec{Y}) - t]e^{-t}\,t^{k-1}. \end{aligned} \qquad (56)$$

Substituting this integral in Eq. (54) and using the fact that $h(\vec{Y})$ is normalized to unity, we get

$$\begin{aligned} \mathrm{Prob.}[M_{k,N} \leqslant w] = 1 &- \frac{1}{\Gamma(k)} \int_0^\infty dt\ e^{-t}\,t^{k-1} \\ &\times \int d\vec{Y}\ h(\vec{Y})\,\Theta[\lambda_N(w,\vec{Y}) - t]. \end{aligned} \qquad (57)$$

Thus interpreting $\lambda_N(w, \vec{Y})$ as a random variable, we get

$$\begin{aligned} \mathrm{Prob.}[M_{k,N} \leqslant w] = 1 &- \frac{1}{\Gamma(k)} \int_0^\infty dt\ \mathrm{Prob.}[\lambda_N(w, \vec{Y}) \geqslant t] \\ &\times e^{-t}\,t^{k-1}, \end{aligned} \qquad (58)$$

where

$$\text{Prob.}[\lambda_N(w, \vec{Y}) \geqslant t] = \int d\vec{Y} \, h(\vec{Y}) \, \Theta[\lambda_N(w, \vec{Y}) - t]. \quad (59)$$

Given the distribution $h(\vec{Y})$ of $\vec{Y}$, it follows that $A(\vec{Y})$ and $\mu(\vec{Y})$ are random variables in Eq. (55). We first need to compute the distribution of $\lambda_N(w, \vec{Y})$ defined in (55) using Eq. (59). Finally, we need to substitute this cumulative distribution function of $\lambda_N(w, \vec{Y})$ in Eq. (58) to compute the cumulative distribution function of $M_{k,N}$. Hence Eq. (58) characterizes the order statistics at the edge for the conditionally independent and identically distributed variables belonging to the Fréchet class.

Let us end this section with the following remark. As discussed above we see that for conditionally independent and identically distributed variables belonging to the Gumbel or Weibull class (but not the Fréchet), one could obtain the statistics of the positions of the particles near the edges by extrapolating the bulk results. One may wonder if the same can be done for independent and identically distributed variables belonging to the Gumbel or the Weibull class. However, it is well known that for independent and identically distributed variables the bulk and the edge order statistics behave very differently and their statistics cannot be derived using just a single framework. Our results demonstrate that, in contrast to the independent and identically distributed case, a single function indeed describes the statistics of the particle positions both in the bulk and at the edges for conditionally independent and identically distributed variables belonging to the Gumbel and the Weibull class.

IV. SIMULTANEOUSLY RESETTING STOCHASTIC PROCESSES

We now provide three concrete physical examples belonging to the three classes where the general results derived above for the conditionally independent and identically distributed variables can be applied. These examples are motivated by the recent advances in the field of stochastic resetting. Stochastic resetting simply means interrupting the natural dynamics of a system (deterministic or stochastic) at random times and restart from the same initial condition. The resetting breaks detailed balance and drives the system to a nonequilibrium stationary state (NESS). This NESS has been studied in various theoretical models [46–61], for recent reviews see Refs. [62–64]. Some of these theoretical predictions have been verified in reent experiments on colloids diffusing in an optical trap [65–67]. As stated in the Introduction, a straightforward and physically interesting way of obtaining conditionally independent and identically distributed variables is through simultaneous resetting of otherwise independent processes. It is a mechanism first introduced in Ref. [32], which we generalize here to two new systems. Specifically, we consider N-independent particles whose positions $X_1(t), \cdots, X_N(t)$ [which we abbreviate as $\vec{X}(t)$] evolve on the line under some dynamics which we refer to as its "natural dynamics." For example, it could be N independent Brownian motions or N independent ballistic particles, etc. For simplicity we consider the evolution in continuous time but this can easily be generalized to discrete time processes such as Lévy flights. We introduce resetting to the origin by

$$\vec{X}(t+dt) = \begin{cases} 0, \ldots, 0 & \text{with probability } rdt \\ \text{each } X_i \text{ evolves independently via its natural dynamics} & \text{with complementary probability } 1 - rdt \end{cases}. \quad (60)$$

In other words, after every time step dt, we either reset all the processes simultaneously to the origin with probability rdt, or we let each process evolve independently, as it would have in the absence of resetting. A cartoon illustrating the trajectories for three particles evolving under this dynamics is shown in Fig. 1. We denote by $p(X \mid \tau)$ the free-propagator (in the absence of resetting) at time τ of this process starting at $X = 0$, i.e., the probability density for the process to arrive at X at time τ, starting at $X = 0$. In the absence of resetting the variables $X_1(\tau), X_2(\tau), \ldots, X_N(\tau)$ are independent. Hence, for a given τ, their joint distribution factorizes $\text{Prob.}[\vec{X} \mid \tau] = \prod_{i=1}^{N} p(X_i \mid \tau)$. We can write a renewal equation for the simultaneously resetting process which reads

$$\text{Prob.}[\vec{X}(t)] = e^{-rt} \prod_{i=1}^{N} p(X_i \mid t) + r \int_0^t d\tau \, e^{-r\tau} \prod_{i=1}^{N} p(X_i \mid \tau). \quad (61)$$

This equation can be understood as follows. There is a possibility that the process never resets in the time interval $[0, t]$. The probability of never resetting in this interval is given by e^{-rt} and the propagator $\prod_{i=1}^{N} p(X_i \mid t)$ gives us the probability for the free process to reach $\vec{X}$ at time t. This corresponds to

the first term of Eq. (61). Otherwise, the process will reset at least once before reaching $\vec{X}$ at time t. Suppose it has reset for the last time at time $t - \tau$, it then has to reach $\vec{X}$ from $\vec{0}$ in the time interval $[t - \tau, t]$ while never resetting. The probability of resetting once is given by $rd\tau$, the probability of never resetting in the interval $[t - \tau, t]$ is given by $e^{-r\tau}$ and the probability of reaching $\vec{X}$ from $\vec{0}$ in time τ is given by the free-propagator $\prod_{i=1}^{N} p(X_i \mid \tau)$. Multiplying this free propagator by the distribution of τ and integrating over τ gives the second term of Eq. (61). We can see from Eq. (61) that in the long time limit, $t \gg 1$, the first term drops out and the simultaneously resetting process reaches a NESS

$$\text{Prob.}[\vec{X}]_{\text{NESS}} = r \int_0^{+\infty} d\tau \, e^{-r\tau} \prod_{i=1}^{N} p(X_i \mid \tau). \quad (62)$$

This steady state is out-of-equilibrium because resetting manifestly breaks detailed balance in the configuration space. Comparing Eq. (2) and Eq. (62) we see that this system provides an example of conditionally independent and identically distributed variables. Here we have only $M = 1$ conditioning variable $Y_1 = \tau$, which is the time elapsed since the last resetting event before t. Since τ has an exponential distribution, we then have $h(\tau) = re^{-r\tau}$ with parameter r. As discussed in

the Introduction, this joint probability density function does not factorize. Indeed the simultaneous resetting induces strong "all-to-all" correlations in our gas.

Given the joint distribution given in Eq. (62) in the NESS, one can investigate various physical observables, such as the average density of the gas, the order statistics, the statistics of gaps between particles or the full counting statistics, i.e., the distribution of the number of particles in a given interval [32]. For example, one of the basic observables is the average density of the gas given by

$$\rho(x, N|r) = \left\langle \frac{1}{N} \sum_{i=1}^{N} \delta(X_i - x) \right\rangle = r \int_0^{+\infty} d\tau \; e^{-r\tau} p(x \mid \tau).$$

(63)

Therefore the average density in the NESS is just the marginal distribution of a set of conditionally independent and identically distributed variables. Interestingly, the average density is independent of N. Similarly the order statistics of the positions of the particles in the NESS of this gas can be derived using the general results for conditionally independent and identically distributed variables detailed before. In this paper, we focus only on the average density and the order statistics, but in principle one can also obtain exactly other observables such as the gap and the full counting statistics.

A. Brownian motion: An example of the Gumbel class

1. The NESS and the average density

In this section, we briefly recall the results of Ref. [32] for the simultaneously resetting Brownian gas. We consider a gas of N simultaneously resetting Brownian walkers on a line evolving via the stochastic dynamics (60); see the left panel of Fig. 1. We will see that this is an example of conditionally independent and identically distributed variables belonging to the Gumbel class. The propagator $p(X \mid \tau)$ of a single particle in the absence of resetting, i.e., the probability density to arrive at X at time τ starting from $X = 0$ is simply diffusive, i.e.,

$$p(X \mid \tau) = \frac{1}{\sqrt{4\pi D\tau}} \exp\left[-\frac{X^2}{4D\tau}\right].$$

(64)

Plugging this propagator in Eq. (62) gives the joint distribution in the NESS

$$\text{Prob.}[\vec{X}]_{\text{NESS}} = r \int_0^{+\infty} \frac{d\tau}{(4\pi D\tau)^{N/2}}$$

$$\times \exp\left[-r\tau - \frac{1}{4D\tau} \sum_{i=1}^{N} X_i^2\right],$$

(65)

which is manifestly nonfactorizable, illustrating the fact that the positions of the particles become correlated in this NESS. The origin of these correlations can be traced back to the simultaneous resetting of the particles [32]. Given this joint distribution, one can compute various observables in principle. For example, the average density in the steady state is given by Eq. (63)

$$\rho(x, N|r) = r \int_0^{+\infty} d\tau \; e^{-r\tau} p(x \mid \tau) = \frac{1}{2}\sqrt{\frac{r}{D}} e^{-\sqrt{\frac{r}{D}}|x|}.$$
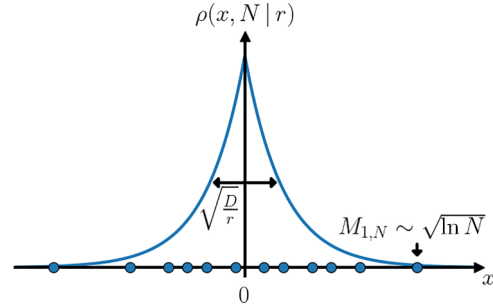
(66)

FIG. 2. The average density $\rho(x, N|r)$, given in Eq. (66), is plotted vs x for N simultaneously resetting Brownian motions with $r = D = 1$. This density is independent of N. The blue dots on the line represent a typical configuration of the particles. The position of the rightmost particle $M_{1,N}$ scales as $\sqrt{\ln N}$ for large N.

Thus, even though at fixed τ the marginal distribution of the conditionally independent and identically distributed variables is Gaussian, once averaged over the conditioning variable τ, the steady-state average density becomes highly non-Gaussian. A plot of this density is shown in Fig. 2.

2. Center of mass

The two first moments of the distribution $p(X \mid \tau)$ are clearly finite and are given by

$$m(\tau) = 0 \text{ and } \sigma^2(\tau) = 2D\tau.$$

(67)

Since $m(\tau) = 0$ we have to use Eq. (19) to obtain the statistics of the center of mass. Plugging Eq. (67) into Eq. (19) we immediately obtain

$$P(C, N) = r \int_0^{+\infty} d\tau \; \sqrt{\frac{N}{4\pi D\tau}} e^{-\frac{NC^2}{4D\tau}} e^{-r\tau} = \frac{1}{2}\sqrt{\frac{rN}{D}} e^{-\sqrt{\frac{rN}{D}}|C|}.$$

(68)

A plot of this scaling function is given in the left panel of Fig. 3 where it is also compared to numerical simulations. Note that this is simply a rescaling of the average density we derived in Eq. (66). This is because in this specific case we actually have a nice trick which allows us to express the center of mass exactly for any N in terms of the density function. Indeed, making use of the fact that Gaussian variables are stable under summation, i.e., if X and Y are Gaussian, then
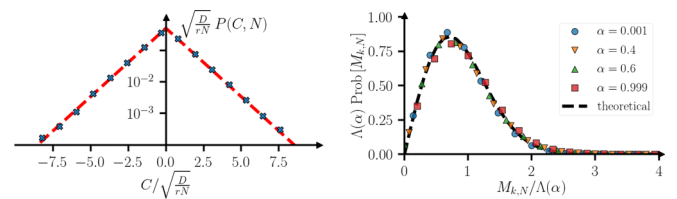

FIG. 3. Plots of the probability density functions of the center of mass (left panel) and the order statistics (right panel) obtained in Eq. (72) and Eq. (75), respectively. The dashed lines correspond to the theoretical predictions in Eq. (72) (left panel) and Eq. (75) (right panel). The symbols represent the results of numerical simulations. Different colors and symbols correspond to different values of $\alpha = k/N$, where we used $N = 1000$.

$X + Y$ is also Gaussian, we can write

$$p(S \mid N\tau) = \int dX_1 \int dX_2 \cdots \int dX_N \, p(X_1 \mid \tau)p(X_2 \mid \tau)$$

$$\cdots p(X_N \mid \tau)\delta(X_1 + X_2 + \cdots + X_N - S)$$

$$= \text{Prob.}\left[\sum_{i=1}^N X_i = S\right], \tag{69}$$

where $S = C N$. This formula can be understood as follows. In order to reach S in time $N\tau$ we split the trajectory into segments of duration τ. Denote by Z_k the position at time $k\tau$ for $0 \leqslant k \leqslant N$. Then telescopically we can write

$$S = Z_N = (Z_N - Z_{N-1}) + (Z_{N-1} - Z_{N-2}) + \cdots + (Z_1 - 0). \tag{70}$$

Then the terms in each parenthesis $X_k = Z_k - Z_{k-1}$ for $1 \leqslant k \leqslant N$ correspond to the distance traveled in the time interval $[(k-1)\tau, k\tau]$. Since Gaussian variables are stable under summation we can split the probability on each of these time segments, leading to Eq. (69). Then we get

$$P(C, N) = rN \int_0^{+\infty} e^{-r\tau} \, \text{Prob.}\left[\sum_{i=1}^N X_i = cN \,\middle|\, \tau\right]d\tau$$

$$= rN \int_0^{+\infty} e^{-r\tau} \, p(CN \mid N\tau) \, d\tau. \tag{71}$$

Changing variable to $y = N\tau$ we get

$$P(C, N) = N\left[\frac{r}{N} \int_0^{+\infty} e^{-\frac{r}{N}y} \, p(CN \mid y) \, dy\right]$$

$$= N\rho\left(CN, N \,\middle|\, r' = \frac{r}{N}\right), \tag{72}$$

where $\rho(x, N|r')$ is precisely the average density in Eq. (66).

3. EVS and order statistics

We now consider the order statistics in the bulk as well as the edge of this gas. The conditional distribution $p(X|\tau)$ in Eq. (64) has a Gaussian tail and hence it clearly belongs to the Gumbel class in Eq. (31). Then, computing the explicit form of the quantile $q(\alpha, \vec{Y}) \equiv q(\alpha, \tau)$ from Eq. (27), we obtain

$$q(\alpha, \tau) = \sqrt{4D\tau} \, \text{erfc}^{-1}(2\alpha), \tag{73}$$

where $\text{erf}(z) = 2/\sqrt{\pi} \int_z^\infty e^{-u^2} \, du$ and $\text{erfc}^{-1}(z)$ is the associated inverse function. As argued in Sec. III B 1, the order statistics in the large-N limit, both in the bulk and at the edges, can be obtained within the same framework, namely from Eq. (30), with the substitution $\vec{Y} \to \tau$ and $h(\vec{Y}) = r \, e^{-r\tau}$. Plugging Eq. (73) in (30) gives

$$\text{Prob.}[M_{k,N} = w] = r \int_0^{+\infty} d\tau e^{-r\tau} \delta[w - \sqrt{4D\tau} \, \text{erfc}^{-1}(2\alpha)]. \tag{74}$$

Performing this integral we immediately obtain

$$\text{Prob.}[M_{k,N} = w] = \frac{1}{\Lambda(\alpha)} f\left[\frac{w}{\Lambda(\alpha)}\right]$$

$$\text{with } \Lambda(\alpha) = \sqrt{\frac{4D}{r}} \text{erfc}^{-1}(2\alpha), \tag{75}$$

where the normalized scaling function $f(z)$ defined on $z > 0$ is given by

$$f(z) = 2 z \, e^{-z^2}, \quad z \geqslant 0, \tag{76}$$

This result was already derived in Ref. [32]. In the right panel of Fig. 3, we compare this analytical prediction to numerical simulations, finding excellent agreement.

B. Random ballistic motion: An example of the Weibull class

1. The NESS and the average density

To find a physical example belonging to the Weibull class of conditionally independent and identically distributed variables, we consider a gas of N particles undergoing ballistic motions on the line. The particles all start at the origin and reset simultaneously to the origin with rate r. At the end of every resetting event, each particle is assigned independently a random velocity v_i drawn from a uniform distribution $n(v)$

$$n(v) = \begin{cases} \frac{1}{2} & \text{if } v \in [-1, 1] \\ 0 & \text{otherwise} \end{cases}. \tag{77}$$

In this case, the free propagator of a single particle at time τ (in the absence of resetting) is given by

$$p(X \mid \tau) = \int_{-\infty}^{+\infty} dv \, \delta(X - v\tau)n(v) = \frac{1}{\tau}n\left(\frac{X}{\tau}\right). \tag{78}$$

An example of the typical trajectories of this system of particles is shown in the middle panel of Fig. 1. Plugging this free-propagator from Eq. (78) into the general formula for the NESS given in Eq. (62), we get

$$\text{Prob.}[\vec{X}]_{\text{NESS}} = r \int_0^{+\infty} d\tau \, e^{-r\tau} \frac{1}{\tau^N} \prod_{i=1}^N n\left(\frac{X_i}{\tau}\right). \tag{79}$$

Once again, the particle positions are strongly correlated in the NESS since the joint distribution does not factorize. Given this exact joint distribution, one can compute various observables, as in the Brownian case. For example, the average density is given by

$$\rho(x, N|r) = r \int_0^{+\infty} d\tau \, e^{-r\tau} p(x \mid \tau) = \frac{r}{2} \int_{r|x|}^{+\infty} \frac{dv}{v} e^{-v}$$

$$= r \, \rho_s(rx), \tag{80}$$

where the normalized scaling function $\rho_s(z)$ defined for $z \in \mathbb{R}$ is given by

$$\rho_s(z) = \frac{1}{2} \int_{|z|}^{+\infty} \frac{dv}{v} e^{-v} = -\frac{1}{2}\text{Ei}(-|z|). \tag{81}$$

Here $\text{Ei}(z)$ is the exponential integral function [68] and the scaling function $\rho_s(z)$ is plotted in Fig. 4. The asymptotics of
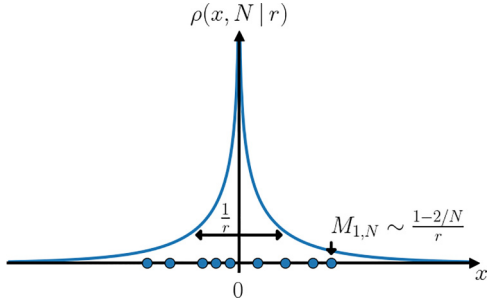
FIG. 4. The average density $\rho(x, N|r)$, given in Eqs. (80) and (81), is plotted vs x for N simultaneously resetting ballistic particles with $r = 1$. This density is independent of N. The blue dots on the line represent a typical configuration of the particles. The position of the rightmost particle $M_{1,N}$ is of order $(1 - 2/N)/r$ for large N.

this scaling function are given by

$$\rho_s(z) \simeq \begin{cases} -\frac{1}{2} \log z & \text{for } |z| \ll 1 \\ e^{-z}/(2z) & \text{for } |z| \gg 1 \end{cases}. \quad (82)$$

2. Center of mass

The first and second moments in this case are also finite and given by

$$m(\tau) = 0, \quad (83)$$

and

$$\sigma^2(\tau) = \int_{-\infty}^{+\infty} dX\, X^2 p(X \mid \tau) - \left[\int_{-\infty}^{+\infty} dX\, X p(X \mid \tau) \right]^2$$

$$= \int_{-\infty}^{+\infty} dX\, \frac{X^2}{\tau} n\left(\frac{X}{\tau}\right)$$

$$= \int_{-\tau}^{+\tau} dX\, \frac{X^2}{2\tau} = \frac{\tau^2}{3}, \quad (84)$$

where we used Eqs. (77) and (78). Since $m(\tau) = 0$ is a constant, independent of τ, we can use Eq. (19) to express the p.d.f. of the center of mass. Plugging Eq. (83) into Eq. (19) we get

$$P(C, N) = r \int_0^{+\infty} d\tau\, \sqrt{\frac{3N}{2\pi\tau^2}} \exp\left[-\frac{3NC^2}{2\tau^2} - r\tau \right]. \quad (85)$$

Changing variable to $\nu = r\tau$ we obtain

$$P(C, N) = \sqrt{\frac{3}{2}Nr^2}\, \ell\left(C\sqrt{\frac{3}{2}Nr^2} \right), \quad (86)$$

where the normalized scaling function $\ell(z)$ defined for $z \in \mathbb{R}$ is given by

$$\ell(z) = \frac{1}{\sqrt{\pi}} \int_0^{+\infty} \frac{d\nu}{\nu} e^{-\nu - z^2/\nu^2}. \quad (87)$$

While this integral does not admit a simple closed form, we can easily compute the asymptotics behaviors, which are given by

$$\ell(z) \to \begin{cases} -\frac{1}{\sqrt{\pi}} \log(z) & \text{for } |z| \ll 1 \\ \left(\frac{\sqrt{3}|z|^{1/3}}{2^{1/3}} \right)^{-1} \exp\left(-\frac{3|z|^{2/3}}{2^{2/3}} \right) & \text{for } |z| \gg 1 \end{cases}. \quad (88)$$
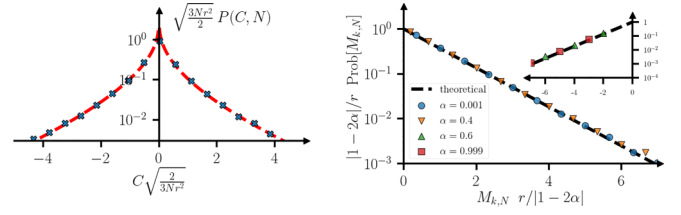

FIG. 5. Left: The scaled distribution of the center of mass. The red dotted lines denote the analytical scaling function $\ell(z)$ in Eq. (87) and the points represent numerical simulations. Right: The distribution of the kth maximum $M_{k=\alpha N, N}$ in the bulk, given in Eq. (92), is plotted on a log-linear scale. In the main figure, we show the curves for $\alpha = 0.001$ and $\alpha = 0.1$ (where the distribution is supported over the positive semiaxis), while the inset shows the curves for $\alpha = 0.6$ and $\alpha = 0.999$ (where the distribution is supported over the negative semiaxis). The black dotted line represent the analytical prediction given in Eq. (92) and the symbols represent simulation results for $N = 1000$ and $r = 1$.

A plot of this normalized scaling function $\ell(z)$ in Eq. (87) is given in the left panel of Fig. 5, where it is also compared to numerical simulations, finding excellent agreement.

3. EVS and order statistics

As in the Gumbel case, one can obtain the distribution of the kth maximum, both in the bulk as well as at the edge, using the same framework leading to Eq. (30), with the substitution $\vec{Y} \to \tau$ and $h(\vec{Y}) = r e^{-r\tau}$. We start by computing the explicit form of the quantile $q(\alpha, \vec{Y}) \equiv q(\alpha, \tau)$. Substituting Eq. (78) in Eq. (27) we obtain

$$\alpha = \int_{q(\alpha, \tau)}^{+\infty} p(X \mid t) dX = \int_{q(\alpha, \tau)}^{+\infty} \frac{dX}{\tau} n\left(\frac{X}{\tau}\right)$$

$$= \int_{q(\alpha, \tau)/\tau}^{+\infty} d\nu\, n(\nu). \quad (89)$$

Using the fact that $n(\nu)$ in Eq. (77) is supported over the finite interval $\nu \in [-1, +1]$, we need to consider three cases: If $q(\alpha, \tau) \leqslant -\tau$, then the integral is equal to 1; if $q(\alpha, \tau) \geqslant \tau$, then the integral is equal to 0 and otherwise we have

$$\alpha = \frac{\tau - q(\alpha, \tau)}{2\tau}. \quad (90)$$

Hence we get

$$q(\alpha, \tau) = \tau(1 - 2\alpha) \quad \text{where} \quad 0 \leqslant \alpha \leqslant 1. \quad (91)$$

The free-propagator, defined in Eq. (78), clearly belongs to the Weibull class in Eq. (38) with $\mu(\vec{Y}) = 1$. Therefore, as discussed in Sec. III B, one can once more replace, for large N, the Gaussian distribution in Eq. (28) by a delta function, leading to Eq. (30) for the order statistics both in the bulk as well as the edges. Plugging Eq. (91) into Eq. (30) we obtain

$$\text{Prob.}[M_{k,N} = w] \approx r \int_0^{+\infty} d\tau\, e^{-r\tau} \delta[w - \tau(1 - 2\alpha)]$$

$$= \frac{r}{|1 - 2\alpha|} \exp\left(-\frac{r|w|}{|1 - 2\alpha|} \right)$$

$$\times \Theta[w(1 - 2\alpha)]. \quad (92)$$

Thus the distribution of the kth maximum $M_{k,N}$, both in the bulk as well as at the edges, is given by an exponential distribution, which is supported on the positive half-line (respectively, negative half-line) for $\alpha < 1/2$ (respectively, for $\alpha > 1/2$), as shown in the right panel of Fig. 5.

C. Lévy Flights: An example of the Fréchet case

1. The NESS and the average density

In this section, we consider a gas of N Lévy flights on the line, all starting at the origin and resetting simultaneously to the origin. Usually Lévy flights (in the absence of resetting) are defined in discrete time where the position of a walker evolves via

$$X_n = X_{n-1} + \eta_n, \quad X_0 = 0, \tag{93}$$

where η_n's are independent and identically distributed random noises with a power-law tail, $p(\eta) \sim |\eta|^{-1-\mu}$ with $0 < \mu < 2$. For large number of steps n, one can replace the discrete time n by a continuous variable τ and it is well known [45] that the free propagator of the Lévy flight for large τ converges to

$$p(X \mid \tau) \approx \frac{1}{\tau^{1/\mu}} \mathcal{L}_\mu\left(\frac{X}{\tau^{1/\mu}}\right), \tag{94}$$

where $\mathcal{L}_\mu(z)$ is the p.d.f. of a centered, normalized to unity, symmetric stable function parametrized by $0 < \mu < 2$. Usually the function $\mathcal{L}_\mu(z)$ is defined by its characteristic function

$$\hat{\mathcal{L}}_\mu(k) = \int_{-\infty}^{+\infty} dz\, e^{ikz} \mathcal{L}_\mu(z) = e^{-|k|^\mu} \quad \text{implying}$$

$$\mathcal{L}_\mu(z) = \int_{-\infty}^{+\infty} \frac{dk}{2\pi} e^{-ikz - |k|^\mu}. \tag{95}$$

A realization of the trajectories for $N = 3$ Lévy flights generated using the propagator in Eq. (94) is shown in Fig. 1 (right panel). Inserting this expression for the free propagator in the general formula for the NESS in Eq. (62), we get the joint distribution of the positions of the simultaneously resetting Lévy flights in the NESS as

$$\text{Prob.}[\vec{X}]_{\text{NESS}} \approx r \int_0^{+\infty} d\tau\, e^{-r\tau} \prod_{i=1}^N \frac{1}{\tau^{1/\mu}} \mathcal{L}_\mu\left(\frac{X_i}{\tau^{1/\mu}}\right). \tag{96}$$

Given this joint distribution, one can compute various physical observables, as in the two preceding cases. In particular, the averaged density is given by

$$\rho(x, N|r) \approx r \int_0^{+\infty} d\tau\, e^{-r\tau} \frac{1}{\tau^{1/\mu}} \mathcal{L}_\mu\left(\frac{x}{\tau^{1/\mu}}\right) = r^{1/\mu} \rho_\mu(r^{1/\mu} x), \tag{97}$$

where the normalized scaling function $\rho_\mu(z)$ is symmetric and is given by

$$\rho_\mu(z) = \mu|z|^{\mu-1} \int_0^{+\infty} du\, \frac{1}{u^\mu} e^{-(|z|/u)^\mu} \mathcal{L}_\mu(u). \tag{98}$$

One can compute the asymptotic behavior of the average density. For large $|z|$, one finds that, for all $0 < \mu < 2$,

$$\rho_\mu(z) \approx \frac{1}{2\pi} \frac{1}{|z|^{1+\mu}}, \quad |z| \to \infty. \tag{99}$$
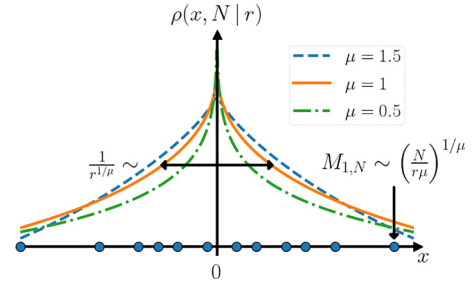
FIG. 6. The average density $\rho(x, N|r)$, given in Eqs. (97) and (98), is plotted vs x for N simultaneously resetting Lévy flights for three different values of $\mu = 0.5$, 1, and 1.5 and $r = 1$. This density is independent of N. For $\mu = 0.5$ and $\mu = 1$, the density diverges as $|z| \to 0$, while it approaches a constant for $\mu = 1.5$. The black dots on the line represent a typical configuration of the particles. The position of the rightmost particle $M_{1,N}$ is of order $N^{1/\mu}$ for large N.

Interestingly, the small-z behavior is quite different depending on the value of μ. Indeed, we get, as $|z| \to 0$,

$$\rho_\mu(z) \approx \begin{cases} \frac{c_1}{|z|^{1-\mu}} & \text{when } 0 < \mu < 1, \\ \frac{1}{\pi}(-\log|z|) & \text{when } \mu = 1, \\ \frac{1}{\mu \sin(\pi/\mu)} & \text{when } 1 < \mu < 2, \end{cases} \tag{100}$$

where we introduced the constant

$$c_1 = \mu \int_0^{+\infty} \frac{dv}{v^\mu} \mathcal{L}_\mu(v). \tag{101}$$

Using $\mathcal{L}_\mu(v) \to O(1)$ as $v \to 0$ [see Eq. (22)], we see that the constant c_1 is well defined for $\mu < 1$. Thus the average density diverges as $|z| \to 0$ for $0 < \mu \leqslant 1$ (but it is still integrable), while it approaches a constant as $|z| \to 0$ for $1 < \mu < 2$. A plot of this density is given in Fig. 6

2. Center of mass

The stable distribution $\mathcal{L}_\mu(z)$ has a power-law tail for large z as in Eq. (22). Hence, the free-propagator in Eq. (94) belongs to the Fréchet class of conditionally independent and identically distributed variables. In this case, for the center of mass $C = \frac{1}{N} \sum_{i=1}^N X_i$, we can use the general result stated in Eq. (20). A straightforward computation, with suitable change of variables leads us to

$$P(C, N) = rN \int_0^{+\infty} d\tau\, e^{-r\tau} \frac{1}{(N\tau)^{1/\mu}} \mathcal{L}_\mu\left[\frac{CN}{(N\tau)^{1/\mu}}\right]. \tag{102}$$

Making a further change of variable $v = N\tau$, one gets

$$P(C, N) = N\left[\frac{r}{N} \int dv\, e^{-\frac{r}{N}v} \frac{1}{v^{1/\mu}} \mathcal{L}_\mu\left(\frac{CN}{v^{1/\mu}}\right)\right]$$

$$= N\rho\left(CN, N\middle|r' = \frac{r}{N}\right), \tag{103}$$

where we used the expression for the average density in Eq. (97). The fact that this distribution of the center of mass is related to the rescaled single-particle propagator can again be traced back to the fact that Lévy variables are stable under addition. Hence the argument used for the Gaussian case in
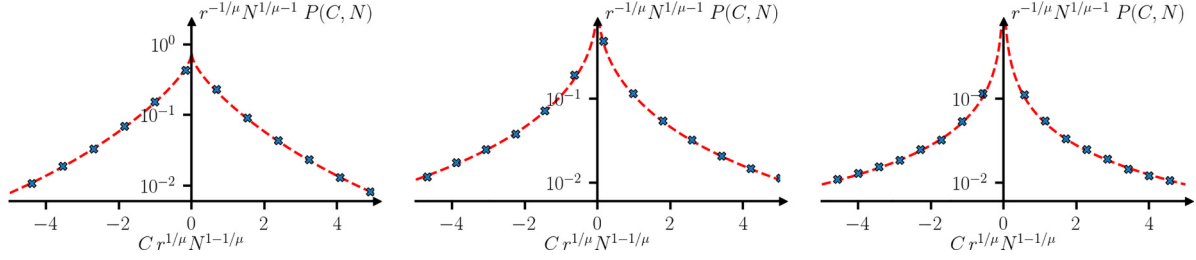
FIG. 7. The p.d.f. of the center of mass $P(C, N)$ in Eq. (104) is shown by dashed lines for $N = 1000$ and for $\mu = 1.5, 1$, and 0.5 in the left, middle, and right panels, respectively. The dots represent numerical simulations.

Eqs. (69)–(72) can also be applied here, explaining the relation in Eq. (103). Finally, from Eqs. (97) and (103) we find that the p.d.f. of the center of mass admits the scaling form for large N

$$P(C, N) \approx N^{1-1/\mu} r^{1/\mu} \rho_\mu(N^{1-1/\mu} r^{1/\mu} C), \quad (104)$$

where $\rho_\mu(z)$ is a symmetric function defined in Eq. (98). A plot of this scaling function is given in Fig. 7 where it is compared to numerical simulations, showing an excellent agreement.

3. EVS and order statistics

Unlike in the two cases (Gumbel and Weibull) discussed before, it turns out that for the Fréchet case, the order statistics in the bulk cannot be extrapolated all the way to the edge. Hence one needs to study separately the statistics of $M_{k,N}$ when $k = \mathcal{O}(N)$ (bulk) and when $k = \mathcal{O}(1)$ (edge).

4. Bulk order statistics

In the bulk, i.e., for $k \sim \mathcal{O}(N)$, we know that the order statistics is given by Eq. (30) with $\vec{Y}$ replaced by τ and $h(\vec{Y})$ replaced by $r e^{-r\tau}$. Hence, we start by computing the explicit form of the quantile $q(\alpha, \vec{Y}) \equiv q(\alpha, \tau)$. Replacing Eq. (94) into Eq. (27) we obtain

$$\alpha = \int_{q(\alpha, \tau)}^{+\infty} p(X \mid \tau) \, dX = \int_{q(\alpha, \tau)}^{+\infty} \frac{1}{\tau^{1/\mu}} \mathcal{L}_\mu\left(\frac{X}{\tau^{1/\mu}}\right) dX. \quad (105)$$

Changing variable to $z = X/\tau^{1/\mu}$ and denoting by $F_\mu(z) = \int_{-\infty}^{z} \mathcal{L}_\mu(x) dx$ the cumulative distribution function of the stable law, we can invert the relation in Eq. (105) and express it as

$$q(\alpha, \tau) = \tau^{1/\mu} F_\mu^{-1}(1 - \alpha) = \tau^{1/\mu} \beta_\mu, \quad (106)$$

where F_μ^{-1} is the inverse function of F_μ. Although we have no closed form for $\beta_\mu = F_\mu^{-1}(1 - \alpha)$, it is simply a constant which we can therefore numerically compute for any practical purpose. Furthermore, from the symmetry of the p.d.f. $\mathcal{L}_\mu(z)$ it follows that if $\alpha < 1/2$, then $\beta_\mu > 0$, while if $\alpha > 1/2$, then $\beta_\mu < 0$. Exactly at $\alpha = 1/2$, $\beta_\mu = 0$. Hence, in the bulk of the system, in the large-N limit, the order statistics will be given by Eq. (30), which can be simplified as

$$\text{Prob.}[M_{k,N} = w] \approx r \int_0^{+\infty} d\tau e^{-r\tau} \delta[w - \tau^{1/\mu} \beta_\mu]$$

$$= \frac{r\mu}{(\beta_\mu)^\mu} w^{\mu-1} \exp\left[-r\left(\frac{w}{\beta_\mu}\right)^\mu\right]$$

$$= \frac{r^{1/\mu}}{\beta_\mu} f_\mu\left(r^{1/\mu} \frac{w}{\beta_\mu}\right), \quad (107)$$

where the normalized scaling function $f_\mu(z)$ defined for $z > 0$ is given by

$$f_\mu(z) = \mu z^{\mu-1} e^{-z^\mu} \theta(z), \quad (108)$$

and is plotted in Fig. 8 for three different values of μ. For $\mu > 1$, the scaling function $f_\mu(z)$ vanishes as $z \to 0$, while for $\mu < 1$ it diverges as $z \to 0$.

5. Edge order statistics

As argued in the general discussion for the Fréchet class in Sec. III B, for the order statistics at the edge, we can no longer use the bulk result in Eq. (30). Instead, we need to use Eq. (58) which holds for any $k = \mathcal{O}(1)$. To proceed, let us first evaluate the large-X behavior of $p(X \mid \tau)$ given in Eq. (94). Using the large-z tail of $\mathcal{L}_\mu(z)$ in Eq. (22) we get

$$p(X \mid \tau) \underset{X \gg 1}{\sim} \frac{\tau}{X^{1+\mu}} \sin\left(\frac{\pi\mu}{2}\right) \frac{\Gamma(\mu+1)}{\pi}. \quad (109)$$

By replacing $\vec{Y}$ by τ and $\mu(\vec{Y})$ by μ in Eq. (43), we see that Eq. (109) is a special case of Eq. (43), namely

$$p(X \mid \tau) \underset{X \gg 1}{\sim} \frac{G\tau}{X^{1+\mu}}, \quad (110)$$

where

$$G = \sin\left(\frac{\pi\mu}{2}\right) \frac{\Gamma(\mu+1)}{\pi}. \quad (111)$$

Then, using Eq. (110) and Eq. (55) it follows that

$$\lambda_N(w, \tau) = \frac{G\tau N}{\mu w^\mu}. \quad (112)$$

Hence the random variable $\lambda_N(w, \tau)$ is proportional to the random variable τ, which itself is distributed exponentially via the p.d.f. $\text{Prob}[\tau] = r e^{-r\tau}$. This leads to

$$\text{Prob.}[\lambda_N(w, \tau) \geqslant v] = \exp\left(-r \frac{\mu v w^\mu}{GN}\right). \quad (113)$$

Plugging this expression in Eq. (58) we then obtain the cumulative distribution function of $M_{k,N}$, which reads

$$\text{Prob.}[M_{k,N} \leqslant w] \approx 1 - \frac{1}{\Gamma(k)} \int_0^{+\infty} dv \, v^{k-1}$$

$$\times \exp\left(-r \frac{\mu v w^\mu}{GN} - v\right)$$

$$= 1 - \frac{1}{[1 + r\mu w^\mu/(GN)]^k} = S_k\left(\frac{r\mu w^\mu}{GN}\right), \quad (114)$$
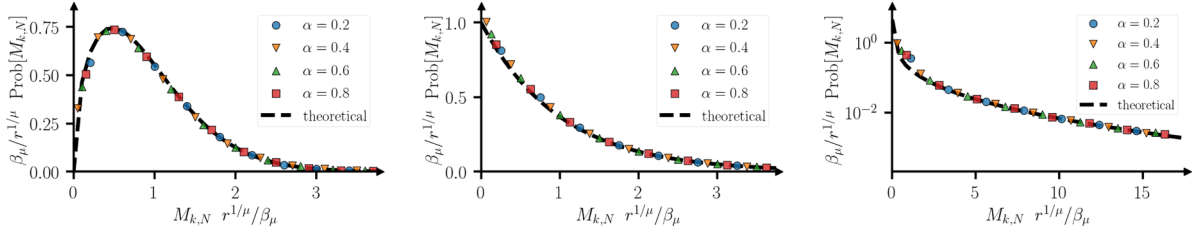
FIG. 8. The p.d.f. of the kth maximum in the bulk $M_{k=\alpha N,N}$ in Eqs. (107) and (108) is shown for $\mu = 1.5$, 1, and 0.5 in the left, middle, and right panels, respectively. Different colors and symbols correspond to different values of k. The dashed black line corresponds to the scaling function in Eq. (107).

where the scaling function $S_k(z)$ defined for $z \geqslant 0$ is given by

$$S_k(z) = 1 - \frac{1}{(1+z)^k}. \tag{115}$$

The p.d.f. is thus given by

$$\text{Prob.}[M_{k,N} = w] = \frac{r\mu^2 w^{\mu-1}}{GN} S_k'\left(\frac{r\mu w^\mu}{GN}\right)$$

$$= \left(\frac{r\mu k}{GN}\right)^{1/\mu} \mathcal{S}_{\mu,k}\left[\left(\frac{r\mu k}{GN}\right)^{1/\mu} w\right], \tag{116}$$

where the normalized scaling function $\mathcal{S}_{\mu,k}(z)$ reads

$$\mathcal{S}_{\mu,k}(z) = \frac{\mu\, z^{\mu-1}}{(1+z^\mu/k)^{1+k}}, \quad z \geqslant 0. \tag{117}$$

For large z, the scaling function decays as a power law $\mathcal{S}_{\mu,k}(z) \sim z^{-1-\mu k}$, while for small z, it behaves as $\mathcal{S}_{\mu,k}(z) \sim z^{\mu-1}$. This scaling function thus characterizes fully the large-N behavior of the order statistics at the edge for simultaneously resetting Lévy flights. In Fig. 9, this scaling function is plotted for three different values of μ in the three panels and compared to numerical simulations, showing a nice agreement.

It is instructive to see how this result connects with the order statistics in the bulk. Taking $k = \alpha N$ and performing the limit $N \to +\infty$ keeping $\alpha \sim \mathcal{O}(1)$ fixed yields

$$\mathcal{S}_{\mu,k}(z) = \mu z^{\mu-1}\left[1 + \frac{z^\mu}{\alpha N}\right]^{-1-\alpha N} \xrightarrow[N \to +\infty]{} \mu z^{\mu-1} e^{-z^\mu} = f_\mu(z). \tag{118}$$

Thus, we recover the scaling function obtained for the order statistics in the bulk given in Eq. (107). The scale factor $r^{1/\mu}/\beta_\mu$ in Eq. (107) for the bulk also matches the scale factor
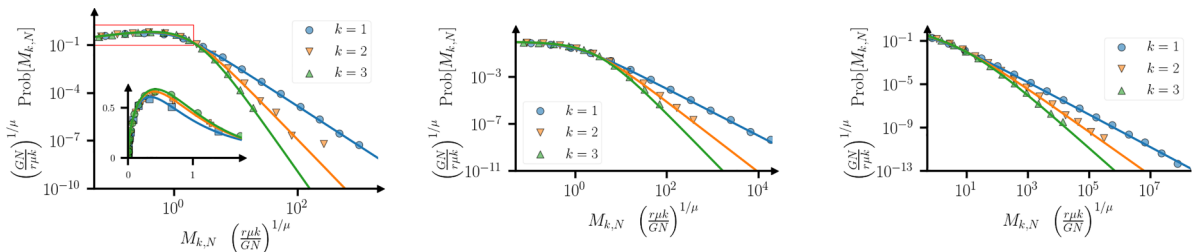
$(\frac{r\mu k}{GN})^{1/\mu}$ in Eq. (116) at the edge. To see this, we first evaluate β_μ in Eq. (106). We get

$$\beta_\mu = F_\mu^{-1}(1-\alpha), \tag{119}$$

which is equivalent to

$$\alpha = \int_{\beta_\mu}^{+\infty} \mathcal{L}_\mu(z)\, dz. \tag{120}$$

In the $\alpha \ll 1$ limit, we can see that $\beta_\mu \gg 1$ and therefore we can use the large-z asymptotics of $\mathcal{L}_\mu(z)$ of the stable distribution given in Eq. (22) inside the integral. Then,

$$\alpha \approx \int_{\beta_\mu}^{+\infty} \frac{G}{z^{1+\mu}}\, dz = \frac{G}{\mu}(\beta_\mu)^{-\mu}, \tag{121}$$

which yields

$$\beta_\mu \approx \left(\frac{G}{\mu\alpha}\right)^{1/\mu} = \left(\frac{GN}{\mu k}\right)^{1/\mu}, \tag{122}$$

where we used $\alpha = k/N$. The scale factor in Eq. (107) is given by

$$\frac{r^{1/\mu}}{\beta_\mu} \xrightarrow[\alpha \ll 1]{} \left(\frac{r\mu k}{GN}\right)^{1/\mu}. \tag{123}$$

Hence the scale factors in the bulk and at the edge clearly match in this limit $\alpha \to 0$.

V. CONCLUSION

In this paper, we have studied the statistics of the scaled sum and the order statistics for a set of N conditionally independent and identically distributed random variables. These

FIG. 9. The p.d.f.'s of the first, second, and the third maximum from the right, i.e., $M_{1,N}$, $M_{2,N}$, and $M_{3,N}$, given in Eqs. (116) and (117) are plotted as solid lines. The three figures correspond to $\mu = 1.5$ (left panel), $\mu = 1$ (middle panel), and $\mu = 0.5$ (right panel). The inset in the left panel shows the behavior close to $z = 0$ where it vanishes as $z^{\mu-1} \sim z^{1/2}$. Different colors and symbols correspond to different values of k.

conditionally independent and identically distributed variables are independent and identically distributed variables for a fixed value of a common parameter (or a set of parameters), but they get correlated when one averages over the distribution of the parameters. This provides a general mechanism to generate a large class of strongly correlated random variables that are still solvable, despite the presence of strong correlations. We studied the analog of the central limit theorem for the scaled sum and also the analog of the three standard classes of extreme value statistics. We showed that averaging over the parameters drastically changes the behavior of these conditionally independent and identically distributed observables compared to the independent and identically distributed case. As a physical example, we considered N simultaneously resetting processes on a line where the resetting dynamics makes them strongly correlated but of the conditionally independent and identically distributed variety. We showed that when the underlying resetting process is Brownian, this corresponds to the Gumbel class of conditionally independent and identically distributed variables. We introduced a new model of independent ballistic particles with random velocities, which corresponds to the Weibull class of conditionally independent and identically distributed variables. Finally, we considered N simultaneously resetting Lévy flights on a line, which corresponds to the Fréchet class of conditionally independent and identically distributed variables. In all these cases, we obtained exact results in the large-N limit for the distribution of the center of mass (i.e., the scaled sum), as well as for the distribution of the kth maximum (i.e., the order statistics).

Here we only considered the statistics of the center of mass and the kth maximum. Using the formalism developed here, one can extend this study to other observables for conditionally independent and identically distributed variables, e.g., to the gap between successive particles or the full counting statistics, i.e., the distribution of the number of particles in a given fixed interval. For N simultaneously resetting Brownian motions (Gumbel class), these other observables have been studied recently in Ref. [32] and it would be interesting to extend these studies to the other two classes, i.e., for the Weibull and the Fréchet class. Another interesting direction would be to study these three models in higher dimensions. Furthermore, a special case where the random variables $\vec{X}$ are conditionally independent and identically distributed when conditioned on $\vec{Y}$ and the random variables $\vec{Y}$ are themselves conditionally independent and identically distributed when conditioned on $\vec{Z}$ might be worth investigating. This hierarchical conditional independence can be iterated and a nice physical example which could be described by this kind of construction is the generalized random energy model introduced in Ref. [24].

VI. APPENDIX

In this Appendix, we derive how the central limit theorem of independent and identically distributed variables generalizes for conditionally independent and identically distributed variables. We start by recalling some main results for the sum [42] and the EVS of independent and identically dis-

tributed random variables [22,43]. We will generalize these to conditionally independent and identically distributed random variables in the following sections. Perhaps the most well-known result for independent and identically distributed random variables is the CLT that characterizes the distribution of the scaled sum of N independent and identically distributed random variables in the large-N limit. Let us consider a set of N independent and identically distributed variables $X_1, \cdots, X_N$ each distributed via the p.d.f. $p(X)$ that has a finite first and second moment

$$m = \langle X_i \rangle = \int X \, p(X) dX \qquad (124)$$

and

$$\sigma^2 = \langle X_i^2 \rangle - \langle X_i \rangle^2 = \int X^2 p(X) dX - \left[\int X \, p(X) dX \right]^2, \tag{125}$$

where the integrals are over the support of $p(X)$. The CLT states that, for large N, the rescaled sum (which we refer to as the "center of mass") $C = \frac{1}{N} \sum_{i=1}^{N} X_i$, converges to a Gaussian distribution, i.e.,

$$P(C, N) \xrightarrow[N \to +\infty]{} \sqrt{\frac{N}{2\pi\sigma^2}} \exp\left[-N\frac{(C-m)^2}{2\sigma^2}\right], \qquad (126)$$

centered at m with a variance σ^2/N. When the p.d.f. $p(X)$ has a diverging second moment, e.g., when $p(X)$ is heavy tailed such as $p(X) \sim X^{-1-\mu}$ for large X with $0 < \mu < 2$, the centered and scaled sum converges to a Lévy stable law with index μ [42].

A. The scaled sum of conditionally independent and identically distributed variables

In this subsection we calculate the general expressions for the distribution of the sum of conditionally independent and identically distributed variables in the large-N limit. We find that, in contrast to independent and identically distributed variables, conditionally independent and identically distributed variables in general do not reach universal limit laws akin to the CLT or its generalizations to Lévy stable laws. We start with the joint distribution in Eq. (15). The p.d.f. of the sample mean, or equivalently the center of mass, $C = \frac{1}{N} \sum_{i=1}^{N} X_i$, can be written as

$$P(C, N) = \int d\vec{X} \, \delta\left(C - \frac{1}{N} \sum_{i=1}^{N} X_i\right) \int \left\{ \prod_{i=1}^{N} p(X_i|\vec{Y}) \right\} \times h(\vec{Y}) d\vec{Y}. \tag{127}$$

Taking the Fourier transform with respect to C, one gets

$$\hat{P}(k, N) = \int P(C, N) e^{ikC} dC = \int d\vec{Y} \left[\hat{p}\left(\frac{k}{N}\Big|\vec{Y}\right) \right]^N$$
$$\times h(\vec{Y}), \qquad (128)$$

where $\hat{p}(k|\vec{Y})$ is the Fourier transform of the conditional distribution function $p(X|\vec{Y})$ with respect to X.

To analyze the large-N behavior of $\hat{P}(k, N)$ in Eq. (128), we need to analyze the small-k behavior of $\hat{p}(k|\vec{Y})$. Let us assume that $p(X|\vec{Y})$ admits a finite first and second moment,

$$m(\vec{Y}) = \int dX \, X \, p(X|\vec{Y}) \text{ and } \sigma^2(\vec{Y})$$
$$= \int dX \, X^2 \, p(X|\vec{Y}) - \left[\int dX \, X \, p(X|\vec{Y}) \right]^2. \quad (129)$$

Then the logarithm of its Fourier transform admits the small-k expansion,

$$\log \hat{p}(k|\vec{Y}) = i \, m(\vec{Y}) \, k - \frac{\sigma^2(\vec{Y})}{2} k^2 + O(k^3). \quad (130)$$

Consequently, exponentiating Eq. (130) and keeping terms up to order $O(k^2)$ inside the exponential, one gets

$$\hat{p}(k|\vec{Y}) \sim e^{i m(\vec{Y}) k - \frac{1}{2}\sigma^2(\vec{Y})k^2}. \quad (131)$$

Substituting this in Eq. (128), and inverting the Fourier transform, we get, for large N,

$$P(C, N) \approx \frac{1}{2\pi} \int_{-\infty}^{\infty} dk \int d\vec{Y} \, e^{im(\vec{Y})k - \frac{1}{2N}\sigma^2(\vec{Y})k^2 - ikC} h(\vec{Y}). \quad (132)$$

If $m(\vec{Y})$ is a nonconstant function of $\vec{Y}$, then we can drop the quadratic term $O(k^2/N)$ in Eq. (132). Then, to leading order for large N, the distribution $P(C, N)$ becomes independent of N with a limiting form

$$P(C, N) \underset{N \to \infty}{\longrightarrow} \int d\vec{Y} \, \delta[m(\vec{Y}) - C] \, h(\vec{Y}). \quad (133)$$

In particular, the moments of this limiting distribution can be calculated easily from Eq. (133) leading to

$$\langle C^n \rangle \underset{N \to \infty}{\longrightarrow} \int d\vec{Y} m^n(\vec{Y}) h(\vec{Y}). \quad (134)$$

On the other hand, if $m(\vec{Y}) = m$ is a constant, then one can shift C by m and rescale it by $\sqrt{N}$. It is then easy to see that $P(C, N)$ converges to a scaling form

$$P(C, N) \underset{N \to \infty}{\longrightarrow} \sqrt{N} \, \mathcal{P}[(C - m)\sqrt{N}], \quad (135)$$

where the scaling function $\mathcal{P}(Z)$ is given by

$$\mathcal{P}(Z) = \frac{1}{2\pi} \int_{-\infty}^{\infty} d\tilde{k} \int d\vec{Y} \, e^{-\frac{1}{2}\sigma^2(\vec{Y})\tilde{k}^2 - i\tilde{k}Z} h(\vec{Y}). \quad (136)$$

Performing the integral over $\tilde{k}$, one finds

$$\mathcal{P}(Z) = \frac{1}{\sqrt{2\pi}} \int \frac{d\vec{Y}}{\sigma(\vec{Y})} \, \exp\left[-\frac{Z^2}{2\sigma^2(\vec{Y})} \right] h(\vec{Y}). \quad (137)$$

This is the main exact result for the limiting distribution of the scaled sum in the case where $m(\vec{Y})$ is independent of $\vec{Y}$. Clearly, the limiting distribution $\mathcal{P}(Z)$ depends on the details of $h(\vec{Y})$ and $\sigma(\vec{Y})$. The moments of the scaling variable Z can be computed from Eq. (137) leading to

$$\langle Z^{2n} \rangle = \frac{\Gamma(2n)}{2^n \Gamma(n)} \int d\vec{Y} \sigma^{2n}(\vec{Y}) h(\vec{Y}), \quad \text{and}$$
$$\langle Z^{2n+1} \rangle = 0 \qquad n = 0, 1, 2 \ldots. \quad (138)$$

Using this result together with the scaling form in (135) we get

$$\langle (C - m)^{2n} \rangle = \frac{\Gamma(2n)}{(2N)^n \Gamma(n)} \int d\vec{Y} \sigma^{2n}(\vec{Y}) h(\vec{Y}), \quad \text{and}$$
$$\langle (C - m)^{2n+1} \rangle = 0 \qquad n = 0, 1, 2 \ldots. \quad (139)$$

So far, we have assumed that the two first moments of $p(X|\vec{Y})$ are finite. In case they are divergent, one can perform a similar analysis for conditionally independent and identically distributed variables as in the case of independent and identically distributed Lévy variables. For simplicity, we assume that the variable X is symmetric with zero mean and the conditional p.d.f. $p(X|\vec{Y})$ has a power-law tail $p(X|\vec{Y}) \sim 1/X^{1+\mu}$ for large X, with $0 < \mu < 2$. We also assume for simplicity that μ is independent of Y. In this case, one can approximate the small-k behavior of the Fourier transform $\hat{p}(k|\vec{Y}) \approx e^{-|b(\vec{Y})k|^\mu}$ where $b(\vec{Y})$ is a scale factor. Substituting this in Eq. (128) and inverting the Fourier transform, we get

$$P(C, N) \approx \int_{-\infty}^{\infty} \frac{dk}{2\pi} \int d\vec{Y} e^{-ikC} e^{-N^{1-1/\mu}|b(\vec{Y})k|^\mu} h(\vec{Y}). \quad (140)$$

Performing the change of variable $k = \tilde{k} N^{1-1/\mu}$, one finds that $P(C, N)$ takes the scaling form

$$P(C, N) \approx N^{1-1/\mu} \, \tilde{\mathcal{P}}_\mu \left(\frac{C}{N^{1/\mu - 1}} \right), \quad (141)$$

where the scaling function $\tilde{\mathcal{P}}_\mu(Z)$ reads

$$\tilde{\mathcal{P}}_\mu(Z) = \int_{-\infty}^{\infty} \frac{d\tilde{k}}{2\pi} \int d\vec{Y} e^{-i\tilde{k}Z} e^{-|b(\vec{Y})\tilde{k}|^\mu} h(\vec{Y}). \quad (142)$$

Finally, performing the integral over $\tilde{k}$, it can be expressed in the compact form

$$\tilde{\mathcal{P}}_\mu(Z) = \int \frac{d\vec{Y}}{b(\vec{Y})} \mathcal{L}_\mu \left[\frac{Z}{b(\vec{Y})} \right] h(\vec{Y}), \quad (143)$$

where $\mathcal{L}_\mu(z)$ is the Lévy stable distribution (scaled to unity) as stated in Eq. (21). In the case $\mu = 2$, $\mathcal{L}_2(z) = e^{-z^2/4}/(2\sqrt{\pi})$ and Eq. (143) gives back (137) with $\sigma(\vec{Y}) = \sqrt{2} \, b(\vec{Y})$.

---

[1] H. Fischer, *A History of the Central Limit Theorem* (Springer, Heidelberg, 2010).

[2] E. J. Gumbel, *Statistics of Extremes* (Dover, Mineola, NY, 1958).

[3] M. R. Leadbetter, G. Lindgren, and H. Rootzen, *Extremes and Related Properties of Random Sequences and Processes* (Springer-Verlag, New York, 1982).

[4] J. Y. Fortin and M. Clusel, Applications of extreme value statistics in physics, J. Phys. A: Math. Theor. **48**, 183001 (2015).

[5] B. C. Arnold, N. Balakrishnan, and H. N. Nagaraja, *A First Course in Order Statistics* (Wiley, New York, 1992).

[6] H. N. Nagaraja and H. A. David, *Order Statistics* (3rd ed.) (Wiley, New York, 2003).

[7] R. W. Katz, M. P. Parlange, and P. Naveau, Statistics of extremes in hydrology, Adv. Water Resour. **25**, 1287 (2002).

[8] P. L. Krapivsky and S. N. Majumdar, Traveling waves, front selection, and exact non trivial exponents in a random fragmentation problem, Phys. Rev. Lett. **85**, 5492 (2000).

[9] S. N. Majumdar and P. L. Krapivsky, Extremal paths on a random Cayley tree, Phys. Rev. E **62**, 7735 (2000).

[10] S. N. Majumdar and P. L. Krapivsky, Extreme value statistics and traveling fronts: Application to computer science, Phys. Rev. E **65**, 036127 (2002).

[11] S. N. Majumdar and P. L. Krapivsky, Extreme value statistics and traveling fronts: Various applications, Physica A **318**, 161 (2003).

[12] S. N. Majumdar, D. S. Dean, and P. L. Krapivsky, Understanding search trees via statistical physics, Pramana, **64**, 1175 (2005).

[13] S. N. Majumdar and J. P. Bouchaud, Optimal time to sell a stock in the Black Scholes model: Comment on 'Thou Shalt Buy and Hold', A. Shiryaev, Z. Xu and X. Y. Zhou, Quant. Financ. **8**, 753 (2008).

[14] P. Embrecht, C. Klüppelberg, and T. Mikosh, *Modelling Extremal Events for Insurance and Finance* (Springer, Berlin, 1997).

[15] B. Derrida, Random energy model: An exactly solvable model of disordered systems, Phys. Rev. B **24**, 2613 (1981).

[16] J. P. Bouchaud and M. Mézard, Universality classes for extreme-value statistics, J. Phys. A: Math. Gen. **30**, 7997 (1997).

[17] I. Weissman, A survey of results on extremes of independent non-identically distributed random variables, Adv. Appl. Probab. **20**, 8 (1988).

[18] C. W. Anderson, Super-slowly varying functions in extreme value theory, J. R. Statist. Soc. **B40**, 197 (1978).

[19] C. W. Anderson, in *Large Deviations of Extremes*, Statistical Extremes and Applications, edited by J. Tiago de Oliveira (Reidel, Dordrecht, 1984), pp. 325–340.

[20] R. A. Davis and S. I. Resnick, Tail estimate motivated by extreme value theory, Ann. Stat. **12**, 1467 (1984).

[21] R. L. Smith and I. Weissman, Large deviations of tail estimated based on the Pareto approximation, J. Appl. Probab. **24**, 619 (1987).

[22] S. N. Majumdar, A. Pal, and G. Schehr, Extreme value statistics of correlated random variables: A pedagogical review, Phys. Rep. **840**, 1 (2020).

[23] B. Derrida, A generalization of the random energy model which includes correlations between energies, J. Phys. Lett. **46**, 401 (1985).

[24] B. Derrida and E. Gardner, Solution of the generalised random energy model, J. Phys. C: Solid State Phys. **19**, 2253 (1986).

[25] C. A. Tracy and H. Widom, Level spacing distributions and the Airy kernel, Commun. Math. Phys. **159**, 151 (1994).

[26] C. A. Tracy and H. Widom, On orthogonal and symplectic matrix ensembles Commun. Math. Phys. **177**, 727 (1996).

[27] D. S. Dean and S. N. Majumdar, Extreme value statistics of hierarchically correlated variables deviation from Gumbel statistics and anomalous persistence, Phys. Rev. E **64**, 046121 (2001).

[28] S. N. Majumdar and A. Comtet, Exact maximal height distribution of fluctuating interfaces, Phys. Rev. Lett. **92**, 225501 (2004).

[29] S. N. Majumdar and A. Comtet, Airy distribution function: From the area under a Brownian excursion to the maximal height of fluctuating interfaces, J. Stat. Phys. **119**, 777 (2005).

[30] G. Schehr and S. N. Majumdar, Universal asymptotic statistics of maximal relative height in one-dimensional solid-on-solid models, Phys. Rev. E **73**, 056103 (2006).

[31] E. Bertin and M. Clusel, Generalized extreme value statistics and sum of correlated variables, J. Phys. A: Math. Gen. **39**, 7607 (2006).

[32] M. Biroli, H. Larralde, S. N. Majumdar, and G. Schehr, Extreme statistics and spacing distribution in a Brownian gas correlated by resetting, Phys. Rev. Lett. **130**, 207101 (2023).

[33] R. Zwanzig, Rate processes with dynamical disorder, Accounts Chem. Res. **23**, 148 (1990).

[34] C. Beck and E. G. D. Cohen, Superstatistics, Physica A **322**, 267 (2003).

[35] C. Beck and E. G. D. Cohen, Superstatistical generalization of the work fluctuation theorem, Physica A **344**, 393 (2004).

[36] C. Beck, E. G. D. Cohen, and H. L. Swinney, From time series to superstatistics, Phys. Rev. E **72**, 056133 (2005).

[37] A. Y. Abul-Magd, G. Akemann, and P. Vivo, Superstatistical generalizations of Wishart-Laguerre ensembles of random matrices, J. Phys. A: Math. Theor. **42**, 175207 (2009).

[38] S. Nairhita and R. Chakrabarti, Tracer diffusion in a sea of polymers with binding zones: mobile vs. frozen traps, Soft Matter **12**, 8554 (2016).

[39] K. Goswami and R. Chakrabarti, Motion of an active particle with dynamical disorder, Soft Matter **18**, 2332 (2022).

[40] M. V. Chubynsky and G. W. Slater, Diffusing diffusivity: A model for anomalous, yet Brownian, diffusion, Phys. Rev. Lett. **113**, 098302 (2014).

[41] A. V. Chechkin, F. Seno, R. Metzler, and I. M. Sokolov, Brownian yet non-Gaussian diffusion: From superstatistics to subordination of diffusing diffusivities, Phys. Rev. X **7**, 021002 (2017).

[42] W. Feller, *An Introduction to Probability Theory and Its Applications*, Vol. 1 and 2 (John Wiley & Sons, New York, 1991).

[43] G. Schehr and S. N. Majumdar, Exact record and order statistics ofrandom walks via first-passage ideas, in *First-Passage Phenomena and their Applications*, edited by R. Metzler (World Scientific, 2014), pp. 226–251.

[44] B. V. Gnedenko, Sur la distribution limite du terme maximum d'une serie aleatoire, Ann. Math. **44**, 423 (1943).

[45] J.-P. Bouchaud and A. Georges, Anomalous diffusion in disordered media: Statistical mechanisms, models and physical applications, Phys. Rep. **195**, 127 (1990).

[46] M. R. Evans and S. N. Majumdar, Diffusion with stochastic resetting, Phys. Rev. Lett. **106**, 160601 (2011).

[47] M. R. Evans and S. N. Majumdar, Diffusion with optimal resetting, J. Phys. A: Math. Theor. **44**, 435001 (2011).

[48] L. Kusmierz, S. N. Majumdar, S. Sabhapandit, and G. Schehr, First order transition for the optimal search time of Lévy flights with resetting, Phys. Rev. Lett. **113**, 220602 (2014).

[49] M. R. Evans and S. N. Majumdar, Diffusion with resetting in arbitrary spatial dimension, J. Phys. A: Math. Theor. **47**, 285001 (2014).

[50] S. N. Majumdar, S. Sabhapandit, and G. Schehr, Dynamical transition in the temporal relaxation of stochastic processes under resetting, Phys. Rev. E **91**, 052131 (2015).

[51] S. Reuveni, Optimal stochastic restart renders fluctuations in first passage times universal, Phys. Rev. Lett. **116**, 170601 (2016).

[52] M. Montero and J. Villarroel, Directed random walk with random restarts: The Sisyphus random walk, Phys. Rev. E **94**, 032132 (2016).

[53] A. Pal, A. Kundu, and M. R. Evans, Diffusion under time-dependent resetting, J. Phys. A: Math. Theor. **49**, 225001 (2016).

[54] A. Pal and S. Reuveni, First passage under restart, Phys. Rev. Lett. **118**, 030603 (2017).

[55] D. Boyer, M. R. Evans, and S. N. Majumdar, Long time scaling behaviour for diffusion with resetting and memory, J. Stat. Mech. **2017**, 023208 (2017).

[56] A. Chechkin and I. M. Sokolov, Random search with resetting: A unified renewal approach, Phys. Rev. Lett. **121**, 050601 (2018).

[57] P. C. Bressloff, Diffusive search for a stochastically-gated target with resetting, J. Phys. A: Math. Theor. **53**, 425001 (2020).

[58] R. G. Pinsky, Diffusive search with spatially dependent resetting, Stoch. Proc. Appl. **130**, 2954 (2020).

[59] B. De Bruyne, S. N. Majumdar, and G. Schehr, Optimal resetting Brownian bridges via enhanced fluctuations, Phys. Rev. Lett. **128**, 200603 (2022).

[60] O. Vilk, M. Assaf, and B. Meerson, Fluctuations and first-passage properties of systems of Brownian particles with reset, Phys. Rev. E **106**, 024117 (2022).

[61] E. Bertin, Stochastic resetting of a population of random walks with resetting-rate-dependent diffusivity, J. Phys. A: Math. Theor. **55**, 384007 (2022).

[62] M. R. Evans, S. N. Majumdar, and G. Schehr, Stochastic resetting and applications, J. Phys. A **53**, 193001 (2020).

[63] S. Gupta and A. M. Jayannavar, Stochastic resetting: A (very) brief review, Front. Phys. **10**, 789097 (2022).

[64] A. Pal, S. Kostinski, and S. Reuveni, The inspection paradox in stochastic resetting, J. Phys. A: Math. Theor. **55**, 021001 (2022).

[65] O. Tal-Friedman, A. Pal, A. Sekhon, S. Reuveni, and Y. Roichman, Experimental realization of diffusion with stochastic resetting, J. Phys. Chem. Lett. **11**, 7350 (2020).

[66] B. Besga, A. Bovon, A. Petrosyan, S. N. Majumdar, and S. Ciliberto, Optimal mean first-passage time for a Brownian searcher subjected to resetting: Experimental and theoretical results, Phys. Rev. Res. **2**, 032029(R) (2020).

[67] F. Faisant, B. Besga, A. Petrosyan, S. Ciliberto, and S. N. Majumdar, Optimal mean first-passage time of a Brownian searcher with resetting in one and two dimensions: Experiments, theory and numerical tests, J. Stat. Mech. **2021**, 113203 (2021).

[68] I. S. Gradshteyn and I. M. Ryzhik, *Table of Integrals, Series, and Products* (Academic Press, San Diego, CA, 2014).